

Polyoxometalate based open-frameworks (POM-OFs)

Haralampos N. Miras,* Laia Vilà-Nadal and Leroy Cronin*

Cite this: *Chem. Soc. Rev.*, 2014, 43, 5679

Received 2nd March 2014

DOI: 10.1039/c4cs00097h

www.rsc.org/csr

Polyoxometalate-based open frameworks (POM-OFs) are extended architectures incorporating metal-oxide cluster units and comprise an emergent family of materials with a large diversity of topologies, structural flexibility and functionality at the nanoscale. Not only do POM-OFs present a wide range of configurable structures, but also have a vast array of physical properties which reflect the properties of the various 'modular' molecular inputs. Here we describe the methodologies that can be used to construct POM-OF materials with important catalytic, electronic, and structural properties and discuss the advantages compared to the metal organic framework analogues. We also show that it is possible to construct POM-OF materials and design and/or fine tune their functionality by manipulating the initially generated building block libraries as well as by controlling the self-assembly towards the specific intermediate (POM) species which is the chemical and structural "information" carrier of the targeted POM-OF material.

1. Introduction

Polyoxometalates (POMs) are a diverse class of compounds mainly constructed by molybdenum, tungsten, vanadium and

niobium at their highest oxidation states (+4, +5, +6) due to the appropriate charge density and charge-to-ionic radius ratio which: (i) allows the formation of π -bonds with the O^{2-} ligands; (ii) prohibit infinite polymerization and (iii) allows the adoption of several coordination geometries in their metal-oxo complexes ranging from tetrahedral to pentagonal bipyramid. This coordination flexibility which is associated to the strong

WestCHEM, School of Chemistry, The University of Glasgow, Glasgow, G12 8QQ, UK. E-mail: harism@chem.gla.ac.uk, Lee.Cronin@glasgow.ac.uk



Haralampos N. Miras

Haralampos N. Miras gained his BSc degree in chemistry from Ioannina University and obtained his PhD under the supervision of Prof. T. A. Kabanos at Ioannina University in 2005. From 2005 he worked on pyrazolate-based coordination materials with Prof. R. G. Raptis at the University of Rio Piedras, before commencing a research associate position with Prof. L. Cronin at the University of Glasgow in 2006. In 2010 he was awarded an RSE research fellowship

co-funded by Marie Curie actions and received a Leadership research fellow award from the University of Glasgow in 2013. Since 2014 he has held both an RSE research fellow and a lecturer position at the University of Glasgow. His research interests are focused on polyoxometalate, chalcogenide and coordination chemistry. In particular, he is interested in the assembly of nanosized conductive materials, the design of functional molecule-based devices and the mechanistic elucidation of self-assembled chemical systems.



Laia Vilà-Nadal

Laia Vilà-Nadal was born in Valls, Alt Camp (Spain). She has received BSc degrees in both Chemistry, (2006), and Biochemistry, (2007) and a Master's degree in Theoretical and Computational Chemistry with an outstanding award in 2008 from the Rovira i Virgili University, Tarragona. In 2007 she joined the Quantum Chemistry Group at the same university, where she obtained her PhD degree in 2011 under the supervision of Prof. Josep Maria Poblet and Dr Antonio

Rodríguez-Fortea. Later that year she joined the Cronin Group as a Post-Doctoral Researcher. Her current research aims to take advantage of the intrinsic electronic properties of POMs as switchable molecular semiconductors to be used in the fabrication of nano-electronic devices.

of ring shaped 'Mo-blues' and spherical shaped 'Mo-browns' families, where the building block library is constituted by a set of virtual synthons $\{\text{Mo}_1\}$, $\{\text{Mo}_2\}$, $\{(\text{Mo})\text{Mo}_5\}$, $\{\text{Mo}_8\}$, that are formed in the reaction medium and organized into nano-scaled species of variety of structural features such as balls, wheels, capped wheels and large 'lemon' shaped clusters based on the assembly-rules imposed by the reaction conditions.²² This class of compounds attracted the attention of research groups due to their interesting physical properties and nanoscale size (Fig. 2).

2. Preparation of cluster and lacunary POM-based building blocks

The acid driven assembly of POM clusters by polycondensation of metalate fragments may be hydrolytically reversed in basic solutions. Careful pH control allows the partial disassembly of heteroPOM clusters with addenda site vacancies of precise location and quantity, ranging from monovacant to hexavacant. These lacunary species are derivatives of the fully-occupied (plenary) typical POM motifs. The effective expulsion of $[\text{M}^{\text{VI}}\text{O}]^{4+}$ from a plenary structure increases the negative charge, and consequently the reactivity of the cluster towards electrophiles, which is a key step for the effective interaction with transition metals, lanthanides and metal complexes for the preparation of extended structures (POM-OFs), as we will discuss later. Mono-, di-, and tri-lacunary species of the Keggin cluster may be formed by partial decomposition of the plenary M_{12} species. However, the number of accessible Keggin lacunary species is not limited to simply M_{11} , M_{10} , and M_9 . Isomerism, absolute site specificity in the isomers with inequivalent addenda positions (β , γ , and δ), and relative site specificity in all polyvacant clusters, are variable. The removal of metal centres is typically destabilising the POM clusters, and isomerism frequently accompanies the removal of addenda. Furthermore, the kinetic

product of partial disassembly is often different to the thermodynamic product, meaning that removal of an addenda centre will often be followed by consecutive isomerisation processes until the most stable configuration is attained. The richest class of Keggin lacunary species are the tungstosilicates, for which the various derivatives, and their isomers, are accessible *via* a complex network of competing equilibria. For example the ϵ -Keggin isomer has been proven an unexpectedly valuable building block for the construction of open framework structures. On the other hand, the most stable subset of Wells–Dawson cluster (tungstophosphates, $\{\text{P}_2\text{W}_{18}\}$) structure has a greater number of addenda atoms and isomers than the Keggin structure, just four of the proposed lacunary Wells–Dawson tungstophosphate species have been isolated, each of which is derived from the α -isomer (Fig. 3). There are two monovacant $\{\text{P}_2\text{W}_{17}\}$ species, which differ according to whether the lacunary position is either in the cap (α_2) or in the belt (α_1) positions. A $\{\text{P}_2\text{W}_{15}\}$ trivacant species, which was initially incorrectly characterised as a divacant, lacks an entire triadic cap. The hexavacant species, $\{\text{P}_2\text{W}_{12}\}$, is deficient of one addenda metal from each of the polar caps, and four from the belt region of the cluster. The removal of just two addenda from the cap positions of $\{\text{P}_2\text{W}_{18}\}$ has long been postulated, and has been observed as a derivative of the Wells–Dawson octadecatungstodiarsonate cluster, $\{\text{As}_2\text{W}_{16}\}$, however no such $\{\text{P}_2\text{W}_{16}\}$ phosphotungstate cluster-type has yet been isolated.

The particular stability of lacunary as well as of plenary polyoxotungstate species has led to their widespread employment as oxygen-donor ligands for the complexation of transition metal ions. Indeed, the incorporation of paramagnetic metals into lacunary coordination sites can produce cluster assemblies with interesting magnetic and catalytic properties as well as plethora of extended structural motifs. Thus, the chemistry of transition metal substituted POMs (TMSPs) is one of the most actively researched fields in modern inorganic chemistry.

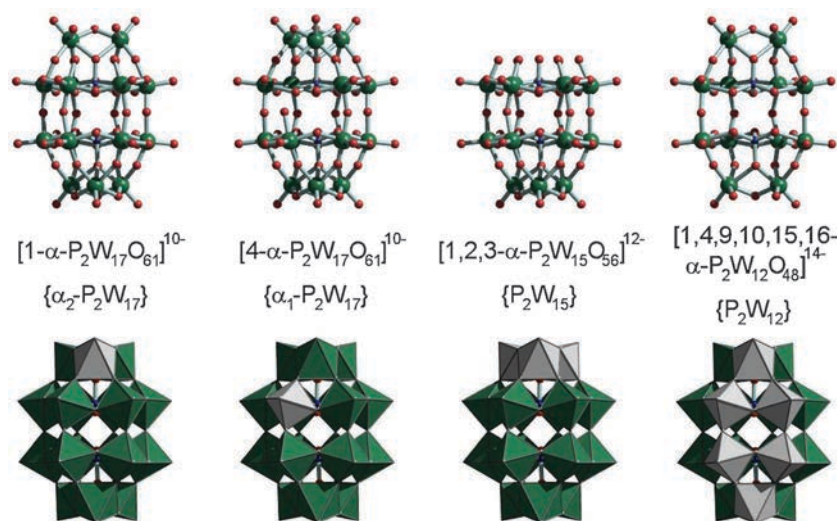


Fig. 3 Accessible lacunary derivative species of the Wells–Dawson octadecatungsto-diphosphate heteropolyanion; two monovacant species, one trivacant species, and a hexavacant species.

The conventional preparation of TMSPs follows a 3-step synthetic pathway: (1) the assembly of the plenary 'parent' POM cluster, (2) the partial disassembly of the parent cluster to form a lacunary species, and (3) the reassembly of a saturated POM species with TM incorporation. The supposed rationale for this strategy is the site specific insertion of the heterometal in step 3, afforded by re-inclusion of an electrophilic centre in the vacancies created by step 2. For a number of species, the direct substitution of TMs for addenda metals has been demonstrated. The number of incorporated TMs is sometimes lower, but usually exceeds the anticipated inclusion by either TM cluster formation or 'out-of-pocket' coordination. Finally, and perhaps most importantly, the insertion of TMs into lacunary POM fragments can also be accompanied by aggregation of clusters to form larger POM-based building blocks or trigger directly the formation of extended architectures. Despite the unpredictable nature of this synthetic strategy, these routes are continually pursued in order to establish a well-defined experimental route. A similar scenario has been observed in the case of phosphotungstate crown-type polyanions, the hexalacunary Wells-Dawson cluster, $\{P_2W_{12}\}$, which has proven an ideal inorganic ligand for the assembly of TMSPs. The large number of addenda vacancies in the cluster ensures that $\{P_2W_{12}\}$ is highly-reactive towards electrophiles. So far, a great variety of clusters ranging

from monomeric to tetrameric have been prepared with $\{P_2W_{12}\}$, incorporating several different TMs (Fig. 4).

A rapid literature examination will show hundreds of examples of lacunary derivative species, we would like to mention here a further example: by means of a conventional 3-step synthesis (followed for the preparation of Keggin-based TMSPs of the W/Mn skeleton), Kögerler *et al.*³¹ synthesised a 4.3 nm manganese(III) polyoxotungstate cluster anion $[Mn_{40}^{III}P_{32}W_{224}^{VI}O_{888}]^{144-}$. The formation of these new $\{Mn_{40}W_{224}\}$ polyanion is defined by a backbone network of dual Mn–O=W bridges. Besides, this is a great example of the unlimited synthetic potential achieved when combining supramolecular templating and kinetic competition approaches in POM synthesis.

Our group has recently showed that is possible to obtain higher nuclearity POMs, with nuclearities ranging from $\{Mo_{36}\}$ to $\{Mo_{368}\}$, in an automated flow-system approach that also allowed us to further expand the POM synthetic potential. Combining an automated flow process with multiple batch crystallizations allowed us to screen and scale up syntheses of POM and Mn-based single molecule magnets.³² The combination of technological control, by means of an automated flow system, and molecular control will certainly be a powerful tool both for the discovery and scale up synthesis of new molecules; in order to have a better yield, determine their properties and finally gain knowledge of their assembly mechanisms.

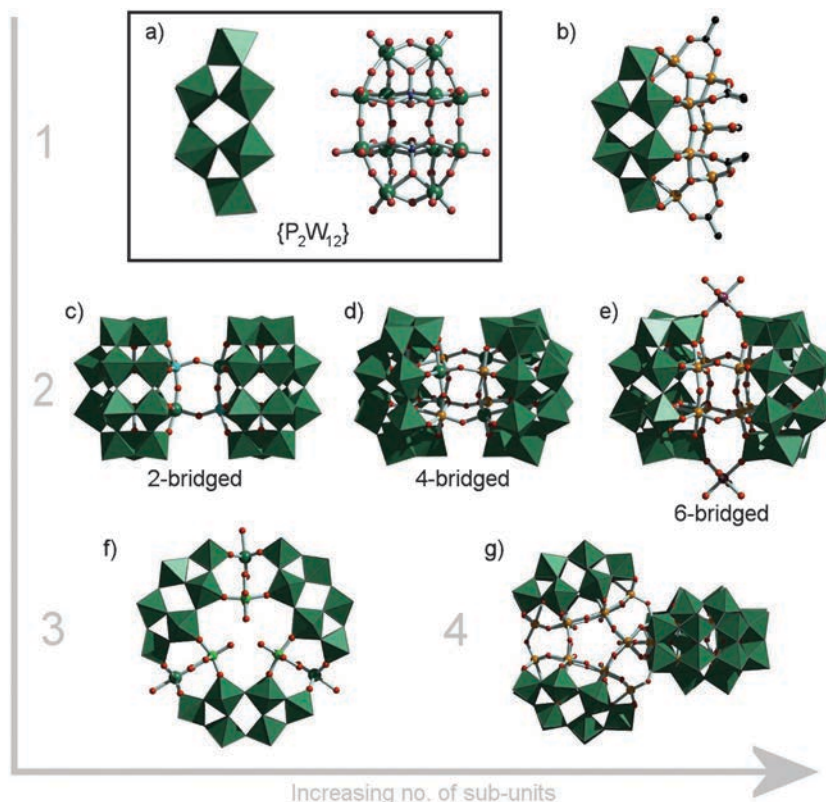


Fig. 4 Selected examples of TMSPs prepared from the hexalacunary $\{P_2W_{12}\}$ building block. (a) The $\{P_2W_{12}\}$ monomer in polyhedral mode from side-on, and face-on in ball and stick mode. (b) The $[H_4P_2W_{12}Fe_9O_{56}(OAc)_7]^{6-}$ monomer.²⁷ (c) The $[\alpha_1-CuP_2W_{17}O_{60}(OH)_2]^{14-}$ dimer with two TM bridges.²⁸ (d) The $[H_{12}P_4W_{28}Fe_8O_{120}]^{16-}$ dimer with four TM bridges.²⁹ (e) The $[(M(H_2O)_4)_2(H_{12}P_4W_{28}Fe_8O_{120})]^{12-}$ dimer with six TM bridges.³⁰ (f) The $[(Mn(H_2O)_4)_2(WO_2(H_2O)_2)_2(WO(H_2O))_3(P_2W_{12}O_{48})_3]^{22-}$ trimer with supplementary W bridges.³⁰ (g) The $[H_yP_8W_{48+x}Fe_{28-x}O_{248}]^{(84-y-3x)-}$ tetramer,²⁷ which has a small number of mixed Fe–W sites.

3. Electronic structure and charge density of POM clusters and building blocks

As mentioned earlier, POM structures are generally formed by metal centres in d^0 or d^1 electronic configurations which are further bonded to O^{2-} ligands producing highly ionic structures. Usually they are considered as very good models of the polymeric metal-oxide phases for the investigation of redox, adsorption and molecular recognition/interaction occurrences with relevance to catalysis and magnetism. The overall negative charge of the molecular metal oxide anions depends on the heteroatom, X (formally P^V , S^{IV} , Al^{III} , I^{VII} ...), and on the oxidation state of the metal centres that constitute the metallic framework. Regardless the overall negative charge, polyoxometalates have available orbitals which can undergo redox processes without major structural rearrangements. This is the reason that reduced POMs species are often referred to as *reservoirs* of electrons, a property which is crucial for the catalytic activity of the prepared POM-OF materials.

POMs in their fully oxidised state are structurally stable in the solid state as well as in solution associated with counter-cations to balance their negative charge. In general, the highest occupied molecular orbitals have p-character while the lowest unoccupied orbitals have metal character. The electronic structure of a fully oxidized POM is quite simple: doubly occupied orbitals (HOMO) are formally delocalized over the oxo ligands and are perfectly separated from the unoccupied set of d-metal orbitals (LUMO). Fig. 5 shows the LUMO of the hourglass-shaped $[S_2W_{18}O_{60}]^{4-}$ anion which is delocalised around the equatorial metals. In Wells–Dawson-type clusters, the first electron is incorporated in the $[M_6O_{18}]$ fragment of the molecular capsule (belt). In this case the LUMO is delocalised over the neighbouring metal centres over the M–O–M bridges. The energy of the LUMO must be low enough to accept the injected electron and the redox properties of a POM are directly related to the energy and composition of the LUMO, as well as the overall cluster architecture. More importantly, the character of the

LUMO's can be manipulated offering an excellent opportunity for fine tuning of the electron transfer/storage process with direct implications in catalysis, batteries and molecular electronics³³ of the POM-based building block, as well as of the designed POM-OF material. For example, the greater electron affinity of tellurium in $[TeW_{18}O_{62}]^{10-}$ modifies the traditional distribution of the LUMO, being mainly localized at the central heteroatom, and therefore the first reduction takes place at the tellurium center. The same situation occurs when iodine is the heteroatom in $[IW_{18}O_{62}]^{9-}$.³⁴ Fig. 5c also depicts the LUMO of the recently published $[Se_8W_{48}O_{176}]^{32-}$ delocalized over the W metal atoms. It has also been observed that in Anderson and Preyssler type anions, not only the M–O–M oxygen atoms but also the X–O–M can be accessed since they present the highest basicity.³⁵ For example the theoretically calculated basic sites in the decavandate $[V_{10}O_{28}]^{6-}$ anion found in agreement with the crystallographic characterization of $[H_3V_{10}O_{28}]^{3-}$.³⁶ On one hand, studies on the $[Mo_6O_{19}]^{2-}$ anion, showed that the Mo–O–Mo is the preferred protonation site. Mapping the electrostatic potential (ESP) over these or even larger building blocks can give an indication of the basic sites which are more susceptible to protonation, as shown in Fig. 6.^{37c}

On the other hand, the geometry, size and oxidation state of the heteroatom has an effect in its neighbourhood electron density area. Consequently, certain properties of the POM can be tuned depending on the heteroatom, *i.e.* the basicity of the protonation sites and also the redox potentials of the metallic shell architecture. That offers an additional means of fine tuning

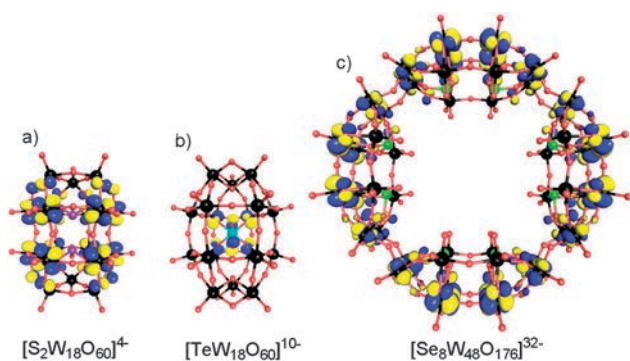


Fig. 5 Representation of the LUMO orbitals of: (a) $[S_2W_{18}O_{60}]^{4-}$, D_{3h} symmetry, delocalized over the belt 5d (W) metal atoms,³³ (b) $[TeW_{18}O_{62}]^{10-}$, D_{3d} symmetry, mainly delocalized over the central heteroatom,^{34,37b} (c) $[Se_8W_{48}O_{176}]^{32-}$, D_{4h} symmetry, delocalized over 5d (W) metal atoms.^{37c} Colour code for spheres and wires, W = black, O = red, S = purple, Te = turquoise, Se = green.

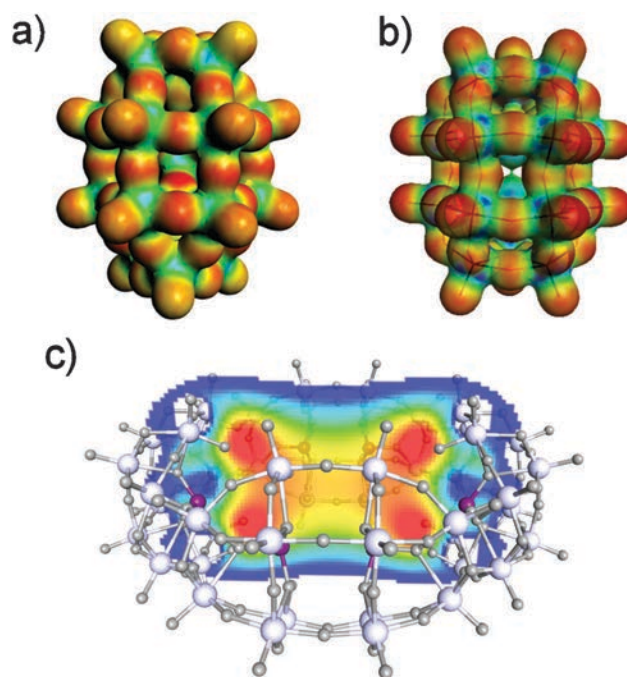


Fig. 6 Computed molecular electrostatic potentials for (a) $[TeW_{18}O_{62}]^{10-}$, (b) $[S_2W_{18}O_{60}]^{4-}$ and (c) the internal region of the wheel-like $[Se_8W_{48}O_{176}]^{32-}$ shown in cross-section through the $\{W_{48}\}$ ring. The most nucleophilic regions can be identified as those shown in red whilst the least nucleophilic regions are mapped in blue.³⁷

the electronic properties of the POM, and consequently the infinite metal oxide derivative, with direct implication in the materials functionality and relevant activity in catalysis, magnetism, battery and fuel cell applications. For further information of *ab initio* calculations on polyoxometalates we recommend a well thought review by Poblet *et al.*^{37a} They have carefully summarized the quantum chemistry studies carried out by several groups over the last 25 years.

4. MOFs vs. POMs: synthetic considerations

Metal-organic frameworks (MOFs) are constructed by combining metal-containing units [secondary building units (SBUs)] with organic linkers, *via* coordination bonds to form open crystalline frameworks with permanent porosity. The variations in coordination modes as well as in the geometry of the metal SBUs and organic linkers led to the synthesis of a plethora of compounds which can be rationally designed on the basis of geometrical grounds.³⁸ In many cases MOFs have excellent porosity which renders them as promising candidates for a wide range of applications such as gas storage, separations, and catalysis. Furthermore, their use in energy related applications such as fuel cells, supercapacitors, and catalytic conversions attracted the attention of numerous research groups as well as the chemical industry. A snapshot of the main crucial developments during the last decade responsible for the advancement of the MOF field are the following: (i) the key role of the geometric considerations and the form of interaction of the SBUs with the organic ligands that forms diverse libraries of various shaped synthons; used for the synthesis of MOFs with specific topology and permanent porosity; (ii) as a natural consequence of the adopted approach, numerous investigations were based on the exploitation of this principle in the design of MOFs with ultrahigh porosity and unusually large pore openings; (iii) the pore functionalization and tuning of reactivity using post-synthetic modifications of pre-synthesized MOFs proven to be a powerful tool for further advances in the chemistry of the MOF family; (iv) multifunctional MOFs, in which multiple organic functionalities are combined within the same framework, opened the door for controllable designing of complexity within the pores of MOFs.

In the conventional synthesis of MOFs usually the reactions are carried out by conventional electric heating. The reaction temperature is one of the main parameters in the synthesis of MOFs, and two temperature ranges, solvothermal (high temperature and pressure) and non-solvothermal, define the type of reaction setups that have to be used. Accordingly, non-solvothermal reactions take place below or at the boiling point under ambient pressure, which simplifies synthetic requirements. Additionally, the solvent is one of the most important parameters in the synthesis of MOFs, which has been investigated to a lesser extent in zeolite synthesis. Although most often no direct interaction with the framework is observed, solvents are almost always incorporated in the as-synthesized MOF structures and thus act as space-filling molecules. Structure-directing agents (SDAs) have been

mostly used in the field of zeolite synthesis, where they act as counterions for charge balance or as templates, in the case of well-defined host-guest interactions. SDAs have also been employed for the preparation of porous MOFs, but it is often hard to identify the role of the solvent as pore-filling molecule (SDA) or as pure reaction medium. One challenge in the use of organic structure-directing agents, such as amines and ammonium ions, is their removal/exchange after the synthesis. This is due to strong host-guest interactions that lead to structural collapse upon removal of the guest molecules. Numerous examples of amine-templated compounds have been described, but most often the removal of the guest molecules was not reported.

From the previous discussion, it becomes apparent that the geometrical control of MOF results from understanding the interplay between the ligand, the metal/cluster nodes and the 'pores', that are always formed as a result of the of building blocks in solution coming together. Further, some of the drawbacks in the synthesis of the MOFs are related to the control of the harsher conditions (high temperature/pressure, prolonged reaction times *etc.*), toxicity of solvents (DMF, DMSO, benzene *etc.*) and removal of structure directing agents from the pores of the MOF. In this respect the synthetic requirements for the assembly of POM based building blocks and consequently POM-OFs usually involve milder conditions (room temperature, atmospheric pressure), innocent solvents (aqueous medium is commonly used), easier counterion exchange, configurable and more diverse architectures based on the generated building block library (Fig. 7). Furthermore, the self-assembly process which drives initially the formation of the POM building block and finally the formation of the POM-OF material offers a few important advantages compared to MOF's synthesis for the following reasons: (1) the intermediate species (POMs) can be well-characterized; (2) the concentration/transformation of the starting materials to the metal-oxide product can be done to identify the pre-existing library of building blocks; (3) the "feedback" obtained from the isolated metal oxide material in terms of architecture or observed properties offers potential for easily designing of the "appropriate" or "desirable" building block library which will lead to the

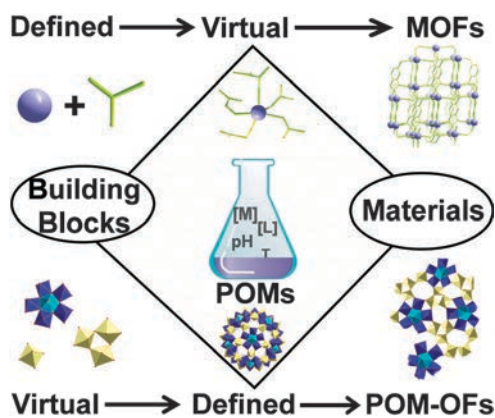


Fig. 7 Comparison of the synthetic approaches for the two families of compounds. Even though the building blocks in MOF synthesis are well defined, the intermediate state is not as opposed to the POM chemistry.

formation of a well-defined, and usually, fully characterized intermediate (POM structure). The building block possess specific structural and chemical information which can be transferred to the final POM-OF material.^{39–43} It is clear that both MOFs and POMF-OFs have different sets of advantages and therefore can be viewed as complementary materials.

5. Extended polyoxometalate open framework assemblies/POM-OFs

5.1 Organic–inorganic hybrids

Pauling's rules for the structures of complex ionic crystals were outlined in his book *The Nature of the Chemical Bond and the Structure of Molecules and Crystals*.^{44,45} These five rules govern the crystal structures of POMs, which generally consist of the large POM anions themselves, along with various cations and solvent molecules. The spatial arrangement of the various POM crystal constituents in the solid state can be of critical importance, and may be considered as the quaternary structure of POMs. Perhaps understandably, the majority of studies on POMs focus on their solution behaviour or the specific characteristics of the polyanionic POM clusters themselves. However, investigations of the properties of POMs in the solid state reveals extremely interesting behaviour and a great opportunity for development of materials with higher degree of control and design.^{46–48} Crystals of large POM anions frequently contain sizeable interstices which accommodate solvent molecules, as well as counterions. More often, the cations occupy regular sites around the POM anion, held in close proximity by electrostatic interactions. However, depending on the degree of charge associated with the cluster anion, there is usually also significant positional disorder of these sites which can be problematical for the structural determination.

Although the components of so called 'POM ionic crystals' are not bonded covalently, as in zeolites and MOFs, such materials

have demonstrated robust porous behaviour. For example, in the work pioneered by Mizuno *et al.*,^{49–51} the combination of anionic POM building blocks with macrocations has produced porous materials with exceptional sorption properties. More specifically they were able to show the ability of the material to adsorb small alcohols and nitriles selectively over longer-chain derivatives, demonstrating the applicability of this material as molecular sieve. The careful selection of both cationic and anionic components is crucial to the structure and properties of the material. For example, the ratio of cation:anion may be controlled by the charge of both components,⁵² while the inclusion of alkyl chains on the cation may increase the hydrophobicity of pores.⁵³ Ionic crystals have also demonstrated heterogeneous catalytic activity in the pinacol rearrangement.⁵⁴ Recently, compounds with unheralded pore sizes have been prepared with bulky organic cations rather than typical macrocationic clusters (Fig. 8). Guest molecules are highly mobile in the pores and can easily be exchanged.⁵⁵

Extensive studies into the solution behaviour of POMs have given chemists a high level of control over the metallic oxo-anions speciation in solution. Therefore, instead of forming simple metal oxide structures, it is possible to use that level of control in the aqueous phase to form more complex, modular metal-oxide structures in the solid state (Fig. 9).⁵⁶ In these rigid POM assemblies, the components are not only held together by the supramolecular interactions considered by Pauling, but typically by coordinative bonds. This means the POMs are incorporated into the framework as integral components in the scaffold, and may be linked into extended one-, two-, or three-dimensional structures through transition metals (TMs), either alone or in combination with intermediary organic moieties, or simply by controlled condensation to generate periodic solid oxides. A number of multi-dimensional compounds containing POMs have been reported, however many non-IUPAC terms have been used, sometimes in a contradictory manner, to describe them.

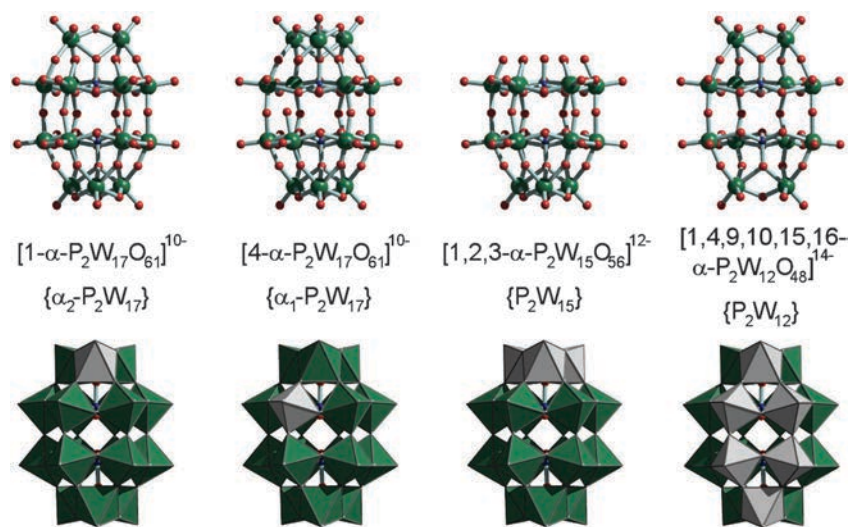


Fig. 8 A highly-porous ionic crystal comprised of (a) the $[\text{Co}_2\text{Zn}_2\{\text{SiW}_{10}\}_2]$ sandwich POM anions, combined with (b) tetrabutylammonium (TBA) cations.⁵⁵ (c) This structure contains spherical $38 \times 38 \times 38 \text{ \AA}^3$ cavities (indicated with blue spheres) in which the guest molecules are highly mobile and may be exchanged. All H atoms and solvent molecules are omitted for clarity.

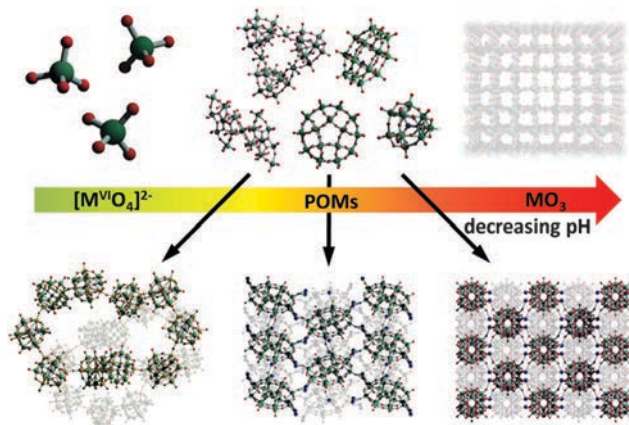


Fig. 9 The acid-driven condensation of metalates to solid oxides can be arrested, allowing the controlled, modular assembly of extended frameworks using POM SBUs.

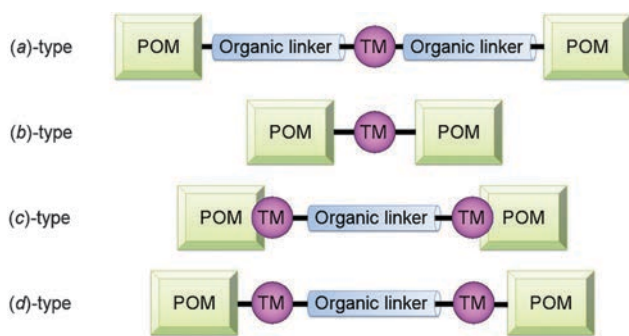


Fig. 10 The four-category classification system of POM frameworks proposed by Cui and Xu: (a) POMs connected to TMs *via* organic units, (b) POMs connected directly to TMs without any organic components, (c) TMSPs connected through organic linkers *via* a heterometal, and (d) POMs connected through organic linkers *via* non-embedded TMs.⁵⁷

One of the main methods adopted for the differentiation between the extended POM assemblies was the nature of the connectivity present in the structure. As part of the main framework scaffold, POMs can be linked in several different ways, typically through transition metals and/or organic moieties. Few attempts have been made to fully categorise POM framework types, however one of the most notable classification systems is the four-category model proposed by Cui and Xu (Fig. 10).⁵⁷ They have proposed that POMs can be linked through a TM centre *via* grafted organic units (a-type), directly through coordinative bonding to a TM centre (b-type), through an organic linker *via* TM sites *within* the POM itself (c-type), and finally through an organic linker *via* TM sites *outwith* the POM cluster (d-type). Each of the connectivity modes are accessed with varying degrees of control, and offer an immense diversity of potential framework architectures.^{58,59}

Utilizing POM-based constituents to manufacture solid-state materials is of great importance not only due to their structural features, but also due to their potential use in different areas of materials science ranging from electrical conductivity and catalysis to magnetism and systems with biological relevance.⁶⁰

Moreover, interesting synergistic effects have also been identified which give rise to emergence of new functionalities and novel phenomena.⁶¹ Based on the previously discussed design approaches suggested by Cui and Xu led to the isolation of a series of interesting solids. The first approach which is based on the grafting of organic moieties on a POM precursor followed by the coupling of organic ligands yielded to a series of materials, namely two examples of dimers of Lindquist type POMs,^{61,62} this is illustrated by the great efficiency of the organoimido derivatives coupling with POMs, catalytic POM terminated dendrimers,⁶³ and polymers with covalently bound POMs.⁶⁴ The remaining two approaches (c and d-type) involve the coordination first of a transition or lanthanide metal with the POM anion followed by a coupling reaction between the two inorganic moieties directly through oxo-bridges or *via* the coordination of a bi- or tridentate organic ligand. The last one (b-type) which does not involve organic linkers led to the formation of few multidimensional architectures.⁶⁵ For example, Dolbecq *et al.* described in 2003^{66a} the preparation of two 1D hybrid organic-inorganic chains with ϵ -Keggin ions as building blocks, namely $[\epsilon\text{-PMo}_{12}\text{O}_{37}(\text{OH})_3\{\text{La}(\text{H}_2\text{O})_4(\text{C}_5\text{H}_6\text{O}_4)_{0.5}\}_4] \cdot 21\text{H}_2\text{O}$ with glutarate ($\text{C}_5\text{H}_6\text{O}_4^{2-}$) linkers and $[\epsilon\text{-PMo}_{12}\text{O}_{39}(\text{OH})\{\text{La}(\text{H}_2\text{O})_6\}_2\{\text{La}(\text{H}_2\text{O})_5(\text{C}_4\text{O}_4)_{0.5}\}_2] \cdot 17\text{H}_2\text{O}$ with squarate ($\text{C}_4\text{O}_4^{2-}$) ligands. These materials were designed according to the third approach mentioned above in Fig. 10. Exploring the reaction conditions that control the assembly of this system, the group managed to prepare a two-dimensional framework $[\text{NC}_4\text{H}_{12}]_2[\text{Mo}_{22}\text{O}_{52}(\text{OH})_{18}\{\text{La}(\text{H}_2\text{O})_4\}_2\{\text{La}(\text{CH}_3\text{COO})_2\}_4] \cdot 8\text{H}_2\text{O}$ see Fig. 11, under hydrothermal conditions. In this case, the basic constituents can be described as double ϵ -Keggin ions capped with lanthanide metal centres. The group demonstrated as well that the dimensionality of the materials can be controlled not only by the reaction variables and the thermodynamics of the system altered by the hydrothermal conditions but also by the nature, the flexibility and the functional groups carried by the organic ligands.

In 2005, the same group reported^{66b} another interesting POM-based open framework architecture based on the same POM-building block and design principles; see Fig. 12. More specifically, they investigated the effect of the processing methodology (mild or hydrothermal conditions) as well as the POM: ligand ratio on the structural motif of the extended frameworks. The Keggin core introduced diversity and its charge the has a direct effect on the architecture of the isolated product; its protonation state as well as the accessible coordination geometries adopted by the capping metal ion are also relevant to the final geometry. This list of variables shows the potential for further design and discovery of fundamentally novel extended frameworks.

In a similar fashion, Mao *et al.*^{66c} utilized the same POM-based building block (ϵ -Keggin) in the presence of Zn^{2+} metal ions, inorganic (PO_4^{3-}) and organic (4,4-bipyridine) linkers to prepare a novel open framework structure with the formula $[\text{CH}_3\text{NH}_3][\text{H}_2\text{bipy}][\text{Zn}_4(\text{bipy})_3(\text{H}_2\text{O})_2\text{Mo}^{\text{V}}\text{Mo}^{\text{VI}}\text{O}_{36}(\text{PO}_4)] \cdot 4\text{H}_2\text{O}$. Four zinc(II) ions coordinate to the Keggin cluster adopting a variety of geometries ranging from tetrahedral to trigonal bipyramidal, and octahedral. The coordination environment of the zinc polyhedron is completed partially by oxygen atoms provided

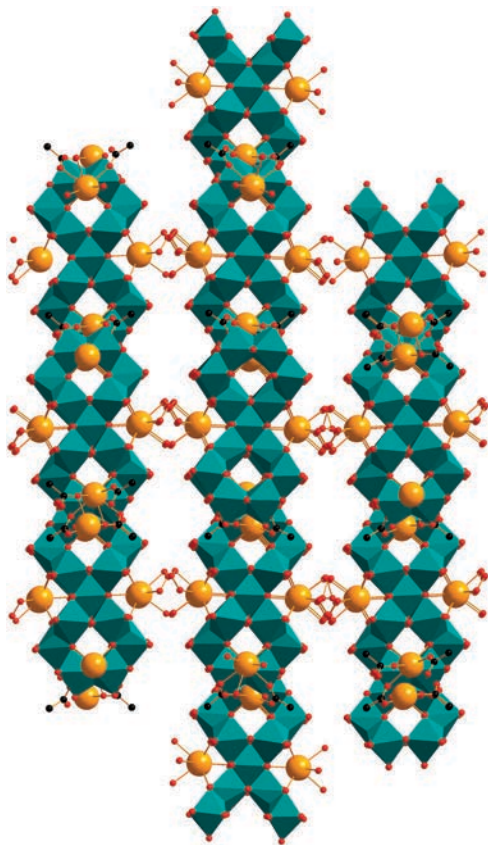


Fig. 11 Representation of the structure of $[\text{NC}_4\text{H}_{12}]_2[\text{Mo}_{22}\text{O}_{52}(\text{OH})_{18} \cdot (\text{La}(\text{H}_2\text{O})_4)_2(\text{La}(\text{CH}_3\text{COO})_2)_4 \cdot 8\text{H}_2\text{O}]$ showing the zigzag chains of $\{\epsilon\text{-PMo}_{12}\}$ ions linked by acetate ligands via the rare earth capping centers. The POM, shown in polyhedral and the rare earth metal centres in ball-and-stick representation. Tetramethyl-ammonium (TMA) cations, and hydrogen atoms are omitted for clarity. Colour code: Mo, teal polyhedra; O, red spheres; La, orange spheres; C, black spheres.

by the Keggin cluster and water molecules, whilst the remaining sites are occupied by nitrogen atoms of the 4,4-bipyridine ligands. Each cluster unit is linked to six neighbouring ones through six 4,4-bipyridine ligands. The two-dimensional sheets are stacked together forming large tunnels along the a axis. These tunnels are occupied by the 1H-protonated methylamine and 2H-protonated 4,4-bipyridine cations and lattice water molecules which provide additional stability to the overall structure.

In 2009 Xu *et al.*⁶⁷ demonstrated the efficacy of the synergistic effect between the POM and the organic constituents of the chemical system, in terms of observed structural topology, but also the effect on the magnetic behaviour. More specifically, the group reported the preparation of two extended inorganic-organic hybrids based on ϵ -Keggin type of molybdo-germanate coordinated to four nickel(II)-organic cations, using both bipyridyl and acyclic amine ligands, $[\text{GeMo}^{\text{V}}_8\text{Mo}^{\text{VI}}_4\text{O}_{36}(\mu\text{-OH})_4\{\text{Ni}(\text{pda})(\text{H}_2\text{O})\}_2\{\text{Ni}(\text{pda})\}\{\text{Ni}(\text{pda})(\text{bpe})\}(\text{bpe})_{0.5}]_n$ and $[\text{GeMo}^{\text{V}}_8\text{Mo}^{\text{VI}}_4\text{O}_{36}(\mu\text{-OH})_4\{\text{Ni}(\text{pda})\}_2\{\text{Ni}(\text{pda})(\text{bpy})_{0.5}\}\{\text{Ni}(\text{pda})(\text{bpy})\}]_n \cdot 7n\text{H}_2\text{O}$ (pda = 1,2-propanediamine, bpe = 1,2-bis(4-pyridine)-ethane, bpy = 4,4'-bipyridine). Both compounds have been synthesized and structurally characterized, and their magnetic properties have also been investigated

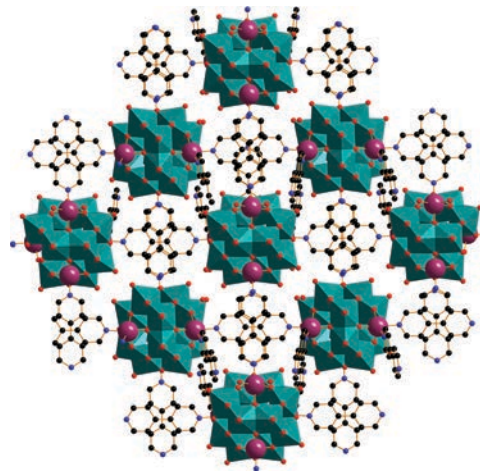


Fig. 12 Representation of the structure of $\text{Na}(\text{C}_{10}\text{H}_{10}\text{N}_2)[\epsilon\text{-PMo}_{12}\text{O}_{40}\text{Zn}_4 \cdot (\text{H}_2\text{O})_2(\text{C}_{10}\text{H}_8\text{N}_2)] \cdot 10\text{H}_2\text{O}$ showing the 2D sheet formed by the connection of ϵ -Keggin units by bipyridine ligands. The POM is shown in polyhedral and the zinc metal centres in ball-and-stick representation. Counterions and hydrogen atoms are omitted for clarity. Colour code: Mo, teal polyhedra; O, red spheres; Zn, purple spheres; C, black spheres.

at temperatures of 2–300 K. The induced intermolecular interactions controlled by the size of the bipyridyl ligand, reflected to the structural features of the extended structure which can be altered from 1D chain to 2D layered sheets.

Very recently, the group of Dolbecq, Kieta *et al.*⁶⁸ expanded further the family of ϵ -Keggin based open frameworks by preparing four new 1D and 2D networks. More specifically, $(\text{TBA})_3\{\text{PMo}^{\text{V}}_8\text{Mo}^{\text{VI}}_4\text{O}_{36}(\text{OH})_4\text{Zn}_4\}[\text{C}_6\text{H}_4(\text{COO})_2]_2$ is a 2D material with monomeric Zn-capped Keggin units connected *via* 1,3 benzenedicarboxylate (isop) linkers and tetrabutylammonium (TBA) counter-cations occupying the space between the planes. In the case of $(\text{TPA})_3\{\text{PMo}^{\text{V}}_8\text{Mo}^{\text{VI}}_4\text{O}_{37}(\text{OH})_3\text{Zn}_4\}[\text{C}_6\text{H}_3(\text{COO})_3] (\text{TPA}[\epsilon(\text{trim})]_\infty)$, 1D inorganic chains formed by the connection of Zn-capped Keggin units which are linked further *via* 1,3,5-benzenetricarboxylate (trim) ligands into a 2D compound with tetrapropylammonium (TPA) cations as counter-cations. In the case of $(\text{TBA})\{\text{PMo}^{\text{V}}_8\text{Mo}^{\text{VI}}_4\text{O}_{40}\text{Zn}_4\}(\text{C}_7\text{H}_4\text{N}_2)_2(\text{C}_7\text{H}_5\text{N}_2)_2 \cdot 12\text{H}_2\text{O}(\epsilon(\text{bim})_4)$ the Zn capped Keggin units are connected to terminal benzimidazole (bim) ligands. Finally, the $(\text{TBA})(\text{C}_{10}\text{H}_{10}\text{N}_4)_2(\text{HPO}_3)\{\text{PMo}^{\text{V}}_8\text{Mo}^{\text{VI}}_4\text{O}_{40}\text{Zn}_4\}_2(\text{C}_{10}\text{H}_9\text{N}_4)_3(\text{C}_{10}\text{H}_8\text{N}_4)(\epsilon_2(\text{pazo})_4)$ is constructed by dimeric Zn capped Keggin units connected by $[\text{HPO}_3]^{2-}$ anions and terminal *para*-azobipyridine (pazo) ligands into overall 1D linear chain. The group also demonstrated a “green” alternative synthetic route for the reduction of graphite oxide (GO) to graphene (G) under mild conditions (room temperature in aqueous solution) using $\epsilon_2(\text{pazo})_4$ and $\epsilon(\text{isop})_2$ as reducing agents. The POM@G obtained material showed enhanced electrochemical properties, large surface area and remarkable stability under various experimental conditions, making them a highly promising class of nanomaterials for a plethora of applications such as photo/electro catalysis, electrode materials and sensors.

The processing methodology used in this system offered an opportunity to control the structural features of the isolated material. More specifically, hydrothermal conditions led to the

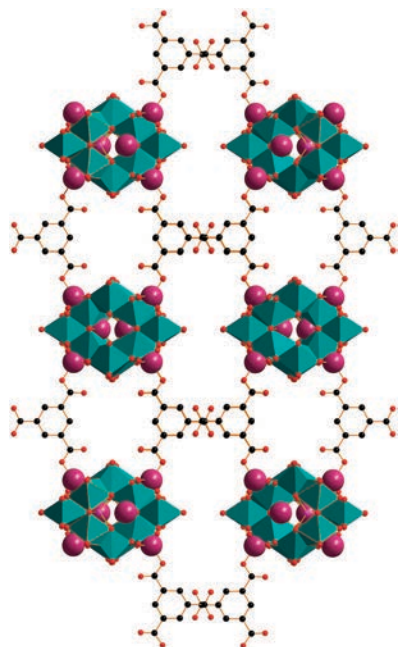


Fig. 13 Representation of the structure of the $(\text{TBA})_3[\text{PMo}^{\text{V}}_8\text{Mo}^{\text{VI}}_4\text{O}_{37}(\text{OH})_3\text{Zn}_4][\text{C}_6\text{H}_3(\text{COO})_3]_3 \cdot 8\text{H}_2\text{O}[\epsilon(\text{trim})]_\infty$ showing the 2D sheet formed by the connection of ϵ -Keggin units by 1,3,5-benzene tricarboxylate ligands; the ϵ -Keggin units, shown in polyhedral and the zinc(II) metal centres in ball-and-stick representation. Counterions and hydrogen atoms are omitted for clarity. Colour code: Mo, teal polyhedra; O, red spheres; Zn, purple spheres; C, black spheres.

grafting of the triangular 1,3,5-benzene tricarboxylate linkers (denoted trim) on tetrahedral ϵ -Keggin polyoxometalates (POMs) capped by Zn(II) ions, which were formed *in situ*, generating three novel POM-based open frameworks.⁶⁹ The most notable example from this effort is the $(\text{TBA})_3[\text{PMo}^{\text{V}}_8\text{Mo}^{\text{VI}}_4\text{O}_{37}(\text{OH})_3\text{Zn}_4][\text{C}_6\text{H}_3(\text{COO})_3]_3 \cdot 8\text{H}_2\text{O}[\epsilon(\text{trim})]_\infty$ extended solid, where zigzag chains are connected *via* the organic moieties into 2D grids; see Fig. 13. Fabrication of modified electrodes by direct adsorption of the isolated material on glassy carbon or entrapment in carbon paste (CPE) showed remarkable electrocatalytic activity for the hydrogen evolution reaction (HER) giving a yield greater than 95%, and a turnover number as high as 1.2×10^5 after 5 h.

Additionally, the $\epsilon(\text{trim})_{4/3}$ and $[\epsilon(\text{trim})]_\infty$ -based electrodes showed equally remarkable behaviour whereby the enclosed environment seems to aid or facilitate the evolution of H_2 gas from aqueous solution, and their performance improved when compared to the ones measured for platinum alone. This performance increase could be explained based on arguments related to the architecture of the open framework materials as well as on the structure associated confinement effect. The confinement effect was hinted at by theoretical investigations, but a clear experimental demonstration is still needed. Also, the demonstration of exceptional electrocatalytic properties shows that neither extensive porosity nor the presence of conjugated system is crucial. This unique feature of POM-OFs materials opens up the door for further promising developments in the field using design approaches for the manufacturing of materials with desired functionalities.

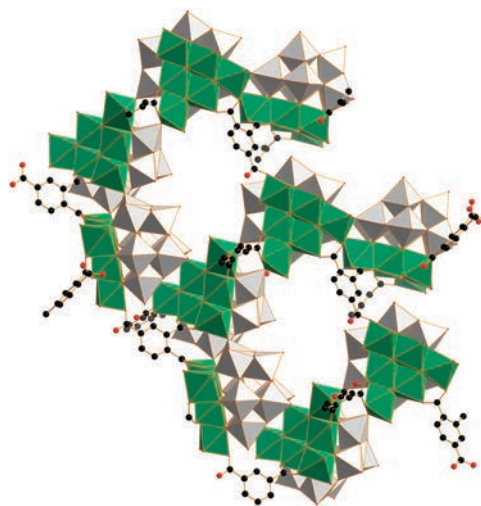


Fig. 14 Structural representation of $\{[\text{Ni}_6(\text{OH})_3(\text{H}_2\text{O})_5\text{PW}_9\text{O}_{34}](1,2,4\text{-btc})\}$ showing the 2D sheet formed by the connection of $\{\text{Ni}_6\text{PW}_9\}$ units by 1,2,4-btc ligands; counterions and hydrogen atoms are omitted for clarity. Colour code: W, grey polyhedra; Ni, green polyhedral; O, red spheres; C, black spheres.

The same group based on their experimental observations as well as theoretical calculations,⁶⁸ made an effort to investigate the effect of imidazole based ligands on the assembly of Zn capped ϵ -Keggin based networked materials. The first attempts led to the isolation of a two-dimensional material, $e(\text{im})_2$. Even though the main building constituent differs from the $\{\epsilon\text{-Zn}_4\text{PMo}_{12}\}$ expected one, $e(\text{im})_2$ contains interconnected anions through imidazolate ligands, demonstrating that the synergistic effect offered by the inorganic and organic units are promising candidates for the development of a new class of imidazole-based POM-based open frameworks.

Utilization of a different POM-based building block by Yang *et al.*⁷⁰ allowed the design and preparation of four novel POM-OFs with 1D and 2D extended structures utilizing a Ni-derivatized lacunary $\{\text{PW}_9\}$ as secondary building unit and rigid carboxylate ligands as linkers under hydrothermal conditions; see Fig. 14. The group demonstrated a reliable and feasible synthetic route which offers a unique opportunity for further design of novel POM-OFs that exhibit interesting magnetic behaviour. The suggested synthetic procedure offers several applications and it can be extended to different combinations of metal substituted POM lacunary structures (*e.g.* $[\text{XW}_{10}\text{O}_{36}]^{n-}$ ($\text{X} = \text{Si}, \text{Ge}, \text{P}$) $[\text{P}_2\text{W}_{12}\text{O}_{48}]^{14-}$, and $[\text{X}_2\text{W}_{15}\text{O}_{56}]^{n-}$ ($\text{X} = \text{P}, \text{As}$)), as secondary building blocks with larger and more rigid carboxylate linkers under hydrothermal conditions.

Recently, the group of Wang *et al.*⁷¹ reported the use of Keggin structures as templates for the assembly of open-framework architectures, namely: $[\text{Cu}(3,4\text{-bpo})_2(\text{H}_2\text{O})(\text{SiW}_{12}\text{O}_{40})] \cdot (3,4\text{-H}_2\text{bpo}) \cdot 7\text{H}_2\text{O}$, and $[\text{Cu}(4,40\text{-Hbpo})_2(4,40\text{-bpo})(\text{H}_2\text{O})(\text{SiW}_{12}\text{O}_{40})] \cdot 3\text{H}_2\text{O}$ ($3,4\text{-bpo} = 2\text{-}(3\text{-pyridyl})\text{-5-(4-pyridyl)}\text{-1,3,4-oxadiazole}$; $4,40\text{-bpo} = 2,5\text{-bis(4-pyridyl)}\text{-1,3,4-oxadiazole}$). X-ray structural analyses revealed that the former compound adopts a two-dimensional (2D) 4,4-grid sheet. The discrete $[\text{SiW}_{12}\text{O}_{40}]^{4-}$ anionic units act as templates, directing the assembly process, as well as stabilizing

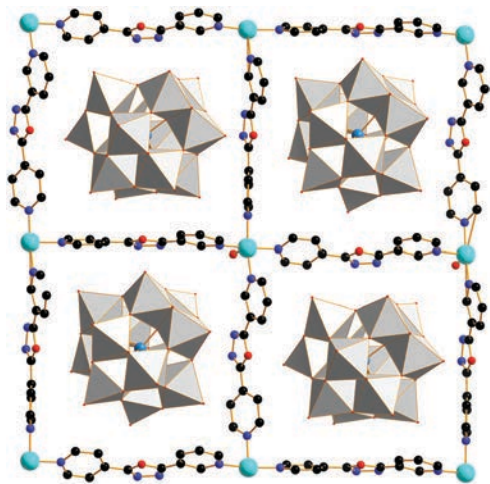


Fig. 15 Representation of $[\text{SiW}_{12}\text{O}_{40}]^{4-}$ arrangement in the 2D grid, counterions and hydrogen atoms are omitted for clarity. Colour code: W, grey polyhedra; Cu, cyan spheres; Si, light blue spheres; O, red spheres; N, blue spheres; C, black spheres.

the overall structure by occupying the formed cavities of the 2D sheet, see Fig. 15. The latter compound exhibits 1D chain structure. The synergistic effect offered by the isomeric organic ligands and the Keggin template play a key role in the observed structural features as well as the self-assembly processes. These two networked structures demonstrate that the rational syntheses by hydrothermal technique can expand the POM-OFs family.

A similar approach was followed recently by Hill *et al.*⁷² to prepare a new POM-OF composite. They used a Cu derivatized phosphotungstic $[\text{Cu}_2\text{PW}_{11}\text{O}_{39}]^{5-}$ POM as template and active constituent. The synergistic effect between the POM units and organic scaffold resulted in enhanced reduction potential of the POM, increased stability of the architecture as well as catalytic activity of the material. The resulting extended solid is catalytically active for the detoxification of various sulphur containing toxic industrial chemicals (H_2S and mercaptans) to elemental sulphur (S_8) and disulphides under ambient conditions (Fig. 16). The catalytic activity of the new POM-OF composite was maintained for at least three cycles without significant activity loss.

Even though, the ϵ -Keggin isomer has been used extensively for the construction of extended solids, examples of structures composed of rare earth elements and saturated heteropolyanions (such as α -Keggin type) are rare. Nevertheless, Wang *et al.*⁷³ reported the preparation of three compounds $[\text{Ln}(\text{NMP})_4(\text{H}_2\text{O})_4][\text{H}_x\text{GeMo}_{12}\text{O}_{40}] \cdot 2\text{NMP} \cdot 3\text{H}_2\text{O}$ ($\text{Ln} = \text{Ce}^{\text{IV}}$; Pr^{IV} , $x = 0$; $\text{Ln} = \text{Nd}^{\text{III}}$, $x = 1$; NMP = *N*-methyl-2-pyrrolidone) in aqueous medium. X-ray diffraction analysis revealed the formation of interesting 2-D supramolecular porous network and extensive hydrogen-bonding interactions between $[\text{M}(\text{NMP})_4(\text{H}_2\text{O})_4]^{3+/4+}$ and $[\text{GeMo}_{12}\text{O}_{40}]^{4-}$ units. Moreover, these compounds showed interesting photochromic properties in the solid state. The crystalline material colour changed from yellow-green to deep brown upon irradiation with mercury lamp for three hours. Interruption of the irradiation induces the opposite colour change. The whole

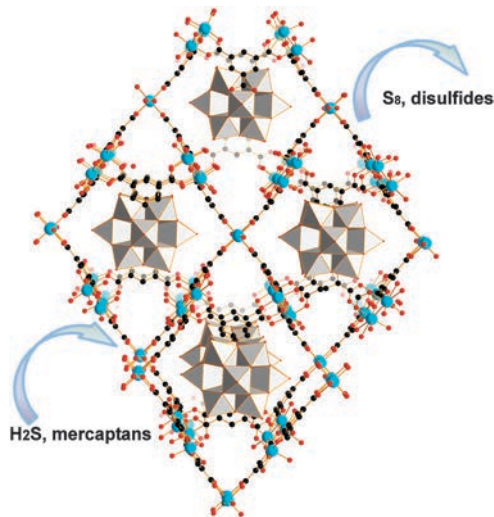


Fig. 16 Representation of the POM-OF composite: POM units, shown in polyhedral representation, are encapsulated orientationally disordered in the pores. The MOF framework is represented in ball and stick form. Tetramethyl-ammonium (TMA) cations, which are disordered in the pores, and hydrogen atoms are omitted for clarity. Colour code: W, grey polyhedra; O, red spheres; Cu, sky blue spheres; C, black spheres.

process is fully reversible which makes these materials excellent candidates for the preparation of photosensing materials.

Furthermore, in 2012, Wu, Li *et al.*⁷⁴ reported a two-step synthetic strategy which led to a new class of layered Mn^{III} -derivatized POM-metalloporphyrin based hybrid materials (Fig. 17). The prepared materials not only revealed interesting complex 2D networked architecture but also showed remarkable selective heterogeneous catalytic activity for the oxidation of alkyl-benzenes with exceptional yields and 100% selectivity. Additionally, the solid materials proved to be excellent scavengers for toxic organic dyes.

In a similar fashion, Cao and co-workers⁷⁵ synthesized an organic-inorganic hybrid solid material based on cucurbituril

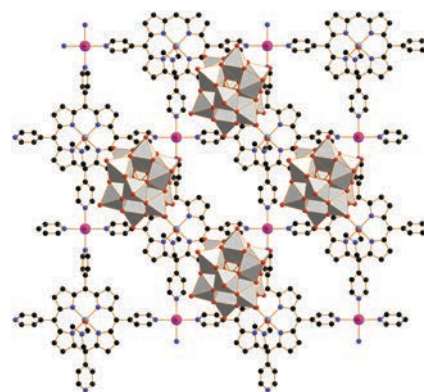


Fig. 17 Representation of the POM-OF composite. View of the single layers of $[\text{Cd}(\text{DMF})_2\text{Mn}^{\text{III}}(\text{DMF})_2\text{TPyP}]_n^{3n+}$ and $[\text{PW}_{12}\text{O}_{40}]^{3-}$ polyanions, along the *c* axis. Colour scheme: Mn^{III} , teal spheres; Cd, pink spheres; $\{\text{WO}_6\}$, light grey octahedra; P, orange spheres; N, blue spheres; C, black spheres. Solvent molecules and H atoms have been omitted for clarity.

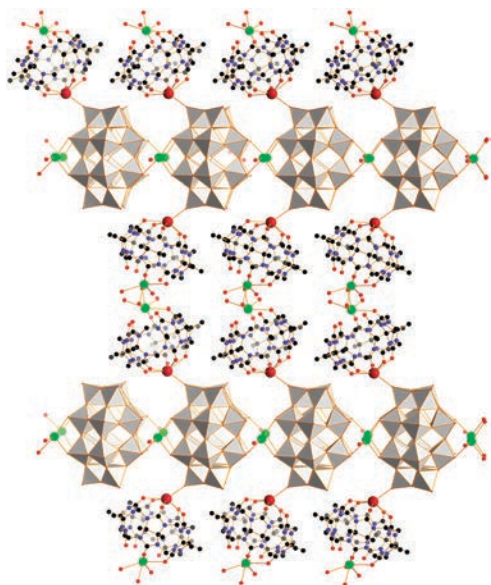


Fig. 18 Representation of the 2D structure of the composite material. The POM structure ($\text{P}_2\text{W}_{18}\text{O}_{62}$) is shown in polyhedral representation while the cucurbituril moieties in ball-and-stick mode. Colour code: W, grey polyhedra; O, red spheres; N, small blue spheres; P, light orange spheres; C, small black spheres; Na, light green spheres; K, red-brown spheres. Protons are omitted for clarity.

derivative and Dawson type polyoxometalate, $\{[\text{K}_2(\text{H}_2\text{O})_2\text{Na}_2(\text{H}_2\text{O})_2\text{Na}_2(\text{H}_2\text{O})_6][\text{P}_2\text{W}_{18}\text{O}_{62}(\text{Me}_{10}\text{Q}_5)_2]\}$ (Fig. 18), which exhibit reversible photochromic properties as well as excellent photocatalytic activity towards the degradation of methyl orange (MO) and rhodamine-B (RB) under visible light irradiation. More specifically, visible light irradiation on a fresh sample resulted in a rapid colour change within 20 min into a dark blue sample. It is possible to reverse reaction to the colourless state could be assisted by heating the material (heating at 50 °C, fast) or letting in the dark (slow, 1 day). Repeated cycling of the described process displayed good reversibility. Moreover, the materials showed excellent photocatalytic activity of methyl orange (MO) degradation under irradiation with visible light. The degradation of MO solution (10 mg L^{-1}) was completed within 180 min.

As mentioned above, apart from the use of transition metals, lanthanides and organic ligands as linkers for the construction of POM-OF networks, several groups adopted an alternative design approach which involves the use of discrete metal complexes as linkers. An interesting representative example of this approach has been reported in 2002 by Zhu, Zhang *et al.*⁷⁶ by using two different type of cobalt complexes, $\text{Co}(\text{en})_2$ and $\text{Co}(\text{bpy})_2$ (en = ethylenediamine; bpy = bipyridine), to link the POM-based moieties ($[\text{PMo}^{\text{VI}}_5\text{Mo}^{\text{V}}_3\text{V}^{\text{IV}}_8\text{O}_{44}]^{6-}$) they obtained a 2D layered extended solid under hydrothermal conditions. This compound also exhibits an antiferromagnetic interaction between metallic centres. The group also demonstrated the value of applying of two types of transition metal complexes as bridges, at the same time, for constructing organic-inorganic hybrid oxide materials.

As an extension to this approach, Gutiérrez-Zorrilla *et al.*⁷⁷ utilized a copper – based dimeric complex, instead of two different

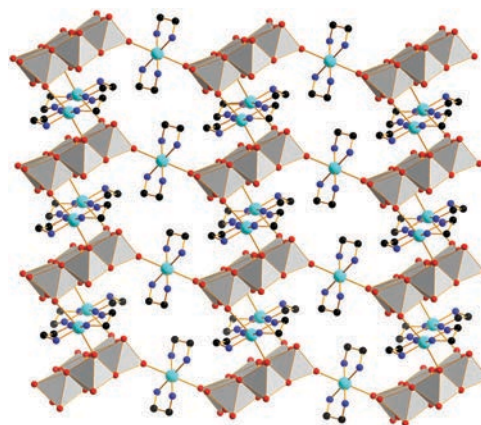


Fig. 19 Representation of the 2D structure of the composite material. The POM structure ($\text{TeMo}_6\text{O}_{24}$) is shown in polyhedral representation while the $\{\text{Cu}(\text{en})_2\}$ complexes in ball-and-stick mode. Colour code: W, grey polyhedra; O, red spheres; N, small blue spheres; C, small black spheres. Counterions and protons are omitted for clarity.

metal complexes, in order to bridge the POM based units. The self-assembly of copper-oxalate dimers and Keggin type polyoxometalates led to the first example of a new class of extended hybrid solids, $\text{K}_{14}\{[\text{Cu}_2(\text{bpy})_2(\mu\text{-ox})]\{\text{SiW}_{11}\text{O}_{39}\text{Cu}(\text{H}_2\text{O})\}\}_2\text{-}[\text{SiW}_{11}\text{O}_{39}\text{Cu}(\text{H}_2\text{O})]\cdot 55\text{H}_2\text{O}$. X-ray diffraction analysis revealed wavy chains built up of alternating $[\text{Cu}_2(\text{bpy})_2(\mu\text{-ox})]^{2+}$ and $[\alpha\text{-SiW}_{11}\text{O}_{39}\text{Cu}(\text{H}_2\text{O})]^{6-}$ building blocks, free $[\alpha\text{-SiW}_{11}\text{O}_{39}\text{Cu}(\text{H}_2\text{O})]^{6-}$ POMs, potassium cations, and hydration water. It is interesting in this case the observation that the Keggin units have dual role; act as building unit for the construction of the 1D chains as well as template for the organization of the 1D chains into an overall 2D extended structure.

The size and the shape of the POM-based constituent can also affect the structural features of the extended solid. Ali *et al.*⁷⁸ reported recently the preparation of two organic-inorganic hybrid tungsten and molybdenum based extended solids, $[\{\text{Na}_4(\text{H}_2\text{O})_{14}\}\text{-}\{\text{Cu}(\text{gly})_2\}]_2[\text{TeMo}_6\text{O}_{24}]$ {gly = glycine} and $[\{\text{Cu}(\text{en})_2\}_3\{\text{TeW}_6\text{O}_{24}\}]\cdot 6\text{H}_2\text{O}$ {en = ethylene-diamine} based on Anderson type heteropolyoxometalates synthesized under hydrothermal conditions; see Fig. 19. In the first case the Anderson type POM moieties are bridged through copper based complexes $\{\text{Cu}(\text{gly})_2\}$ into an overall 1D open rack-like architecture, where the flat structure of the Anderson POM units act as steps and cationic Cu-organic complexes act as handles of the rack. In the case of the extended solid where the linkers are $\text{Cu}(\text{en})_2$ complexes, independent rack-like architectures are further extended into a 2D coordination polymer.

Interestingly, both of the extended solids presented an exceptional thermal stability (~ 400 °C); moreover both compounds found to be effective heterogeneous catalysts for the epoxidation of cyclohexene to epoxides at moderately high yield ($\sim 60\%$), with dialcohol formed by the hydrolysis of epoxides, as the other major product ($\sim 28\%$). This work also shows the potential for design more efficient and/or selective catalysts by modification of these extended solids. The interplay between the incorporated transition metal ions or metal complexes and the POM-based units allows the design of desirable catalytic activity or potentially emergence of functionality.

5.2 All-inorganic POM-OFs

The second class of compounds defined in the four-category system of POM framework classification consists of POMs connected solely through TMs, with organic components either completely absent, or present only as coordinating units which are not part of the main framework scaffold. In these materials, the TM is considered to be a separate entity from the POM *i.e.* the TM does not occupy a well-defined lacunary site in the cluster. As the number of coordination sites on both the POM and the TM can be numerous (and in the case of POMs hard to define), the assignment of node and linker in such architectures is not trivial. These compounds are more commonly observed than the (a)-type frameworks, and due to the lack of an organic component, (b)-type frameworks are generally more thermally stable. The TM centre can also be redox-active, and the oxidation state of the TM linker may be switchable with overall retention of the framework integrity.

An early example of a (b)-type framework was presented by Khan *et al.* in 1999, and displays a regular cubic arrangement of $\{V_{18}\}$ cages linked through either Fe or Co.⁷⁹ Interestingly, the high porosity of this arrangement allows the interpenetration of two frameworks, which is a common phenomenon in MOF chemistry. One further example of a (b)-type framework contains Wells–Dawson clusters linked together through Ni^{2+} cations, with bpp ligands completing the coordination sphere of the Ni^{II} centres. This combination produces a network with Perovskite topology, which is well-known zeolite architecture, indicating that POMs can be arranged into zeolite frameworks. Although the organic ligands play no direct role in the connectivity of the framework components, their presence prevents interpenetration, and therefore helps to retain the highly-porous nature of the framework, Fig. 20.

Another interesting piece of work reported by Mizuno *et al.* involves the assembly of nanocrystallites with great potential for the design of new materials and emergence of properties in the macroscale. The temperature and the type of counterion

used were the key variables for controlling the crystallinity and porosity of all-inorganic dodecatungstophosphate $M_3PW_{12}O_{40}$ (M: Cs, NH_4 , Ag, denoted as MPW) particles. It was demonstrated the self-organization of 5–10 nm nanocrystallites based on the porous $M_3PW_{12}O_{40}$ (M: NH_4 , Cs, denoted as MPW) moieties. Furthermore, the group managed to elucidate the formation and growth mechanism of MPW particles which involves three steps: formation of the nanocrystallites, assembly of the nanocrystallites to form aggregates, and further growth of the aggregates by incorporation of additional nanocrystallites.⁸⁰

Generally for all modular framework materials, the careful selection of building blocks is crucial to both the structural features and properties of the final product. There are two main strategies for maximizing the porosity of a framework; (1) selecting long narrow linkers, which may lead to interpenetration, or (2) including a pore within the building block itself. In a similar fashion, the application of crown-type POMs to construct porous frameworks relies on the latter strategy. Itself constructed by an aggregation of smaller building blocks, the crown-type polytungstophosphate, $\{P_8W_{48}\}$, has proven to be a fruitful secondary building unit (SBU) in the construction of POM framework materials.^{81–85} So far, Co, Mn and Ni have been used to connect $\{P_8W_{48}\}$ rings into frameworks by (b)-type connectivity. Despite the limited library of building blocks, this has resulted in a number of diverse framework topologies. One of the most striking examples of which is the Mn-linked cubic framework, $K_{18}Li_6[Mn_8(H_2O)_{48}P_8W_{48}O_{184}] \cdot 108H_2O$, Fig. 22.⁸⁶ This compound comprises 8-connected $\{P_8W_{48}\}$ rings, fused together through the sharing of multiple Mn^{II} centres, which are coordinated to the external surfaces of the rings. The perpendicular orientation of connected $\{P_8W_{48}\}$ SBUs defines an infinite array of cubic sub-structures, which encloses roughly spherical cavities of approximately 7.2 nm^3 volume. These cavities proved to be accessible through the $\sim 1 \text{ nm}$ diameter $\{P_8W_{48}\}$ pores. In its native state, the vacancies in the framework are occupied by alkali metal cations and solvent water molecules.

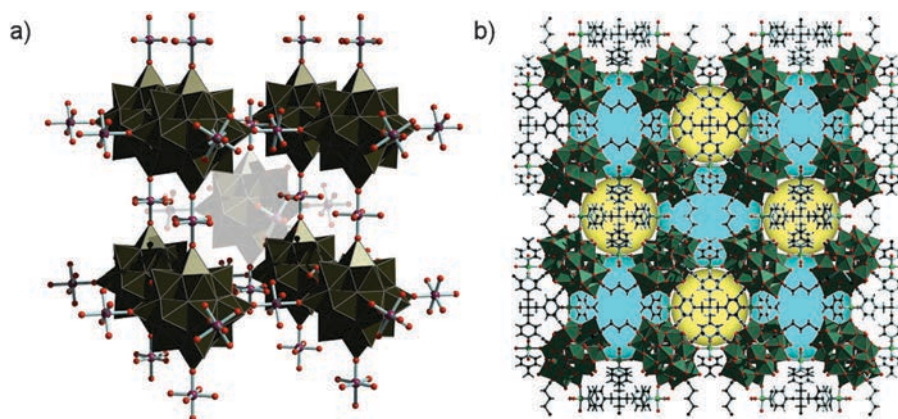


Fig. 20 Two examples of (b)-type POM frameworks, which are connected through TMs without intermediary organic components. (a) A cubic arrangement of $\{V_{18}\}$ clusters linked through Co^{II} centres.⁷⁹ This compound has interpenetration of two frameworks, which is a common phenomenon in MOF chemistry (an interpenetrating cluster is shown faded in the centre). (b) A 3D framework of Wells–Dawson clusters connected through Ni, which has the well-known zeolite structure of Perovskite. Additional ligands on the Ni^{II} centres prevent interpenetration, and define two pore environments of 16.3 \AA diameter (blue) and 13.3 \AA diameter (yellow).

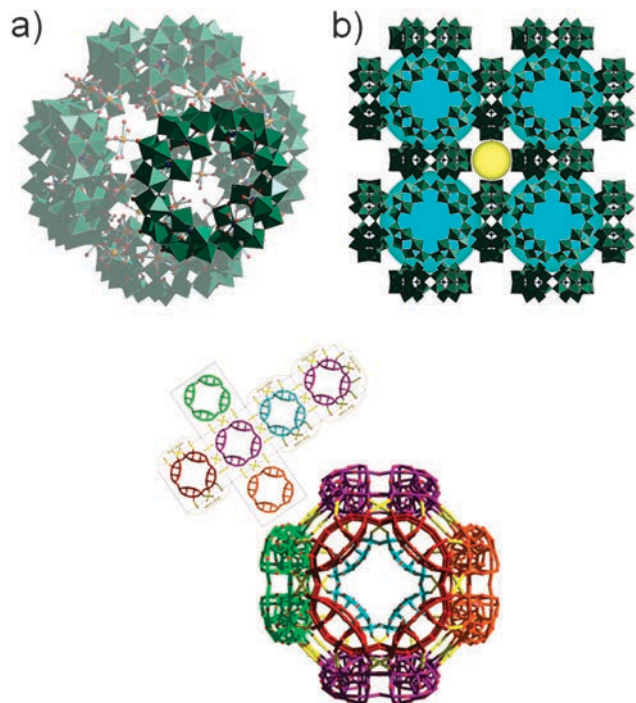


Fig. 21 Top: the Mn-linked cubic framework, $K_{18}Li_6[Mn_8(H_2O)_{48}P_8W_{48}O_{184} \cdot 108H_2O]$.⁸⁶ (a) Individual $\{P_8W_{48}\}$ SBUs are connected through Mn^{II} centres to form a face-directed cube, with internal cavity volume of approximately 7.2 nm^3 ; (b) by sharing faces, the cubes are connected into an infinite three-dimensional lattice. The roughly spherical voids defined by the cubes are indicated in blue, with additional solvent-accessible channels indicated in yellow. All Mn^{II} centres, solvent water molecules and alkali metal cations are omitted for clarity. Bottom: a scheme showing the assembly of the cube with the $\{W_{48}\}$ clusters each colour coded.

The cavity (inside each truncated cuboctahedron ‘box’) is free of heavy metal atoms and, in addition to solvent water molecules, contains only the alkali-metal cations K^+ and Li^+ . Because these cavities are accessible through the ring openings defined by the $\{P_8W_{48}O_{184}\}^{40-}$ units (essentially operating as pores), the cation exchange properties of the material could be monitored through facile cation uptake experiments. The reported studies demonstrated the exchange of K^+ and Li^+ for d-block transition-metal cations, for example Cu^{2+} , Co^{2+} and Ni^{2+} (Fig. 21).

The development of a new synthetic strategy towards a family of transition metal-substituted POMs (TMSPs), continued through the study of POM physical properties in solution, and culminated in the empirical analysis of a new family of structures. TMSPs which are directly connected through their heterometal termini *via* a bridging oxygen atom. For example our group reported recently the directed assembly of the first 3D POM-based framework, $[(C_4H_{10}NO)_{46}(W_{72}Mn_{12}O_{268}X_7)_n]$ ($X = Si$ or Ge) which is based on the substituted Keggin-type POM building blocks and yields a material that can undergo a reversible redox process that involves the simultaneous inclusion of the redox reagent with a concerted and spatially ordered redox change of the framework, Fig. 22.⁸⁷ Furthermore, we have demonstrated that it is possible to construct framework architectures that undergo controlled reversible single-crystal

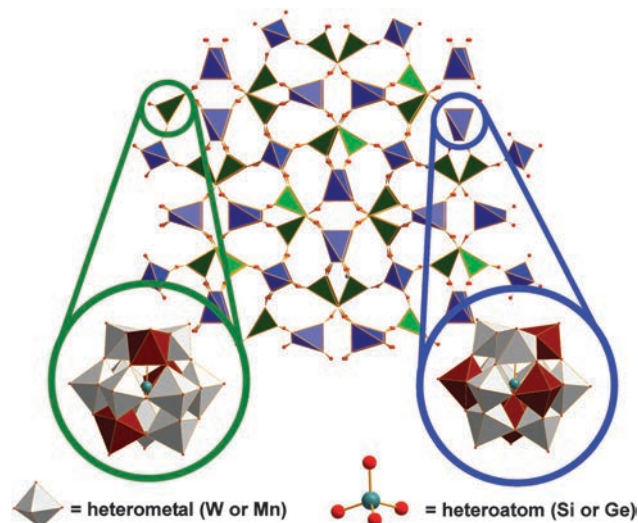


Fig. 22 Representation of the ‘Keggin-net’ structure $(C_4H_{10}NO)_m-[W_{72}M^{II/III}_{12}X_7O_{268}]$ (where $M = Co^{II}$ or Mn^{III} ; $X = Si$ or Ge) constructed from two types of transition-metal-substituted α -Keggin clusters: 4-connected (blue tetrahedra) and 3-connected (green triangles). The overall structure is represented by linked 3- and 4-connected polyhedra with the oxygen linkers (red spheres) and the structure of the 3- and 4-connected Keggin-nodes shown in green and blue insets, respectively. Insets: the ‘modular’ or interchangeable components are shown as cyan polyhedra (the octahedrally coordinated heterometal centre) and teal spheres (the tetrahedrally coordinated heteroatom centre). Colour code: heterometal (Mn or Co), dark red polyhedra; W, grey polyhedra; O, small red spheres; heteroatom (Si or Ge), teal spheres. Counterions and solvent molecules are omitted for clarity.

to single-crystal (SC–SC) redox transformations, where the kinetics of the processes are controlled by the redox agent and the heteroatom embedded within the Keggin moieties. This work showed that it is possible to modify the overall structure following a redox-based ‘post-assembly’ modification. This opens up a plethora of applications whereby redox-tunable frameworks such as those discussed here could be applied as sensors or catalysts. Extending this piece of work, another two new members $\{(C_4H_{10}NO)_{46}[W_{72}Co^{II}_{12}X_7(OH)_6O_{262}]\}_n$ ($X = Si$ or Ge) of the ‘Keggin Net’ family were isolated. The introduction of the cobalt heterometal has altered the redox activity of this family of compounds. The Co^{II} bridging metal centres can be oxidized to less stable Co^{III} analogue in a reversible SC–SC (single crystal to single crystal) transformation in which the framework integrity of the material is completely retained.

Furthermore, the concept of molecular alloys has been realized for the first time in the context of 3D inorganic frameworks and is demonstrated by a series of linked mixed Co–Mn polyoxometalate networks, thus opening up another route to discover new electronically interesting materials with emergent physical properties (*i.e.* a solid solution of Mn and Co ions in the Keggin-network archetype).^{88,89} Further, a similar synthetic strategy which employs other metal ions (M) and heterotemplates (X) should result in the formation of a family of related materials. The combination of the structurally conserved redox switching and the ability to reform the material by repeated dissolution and recrystallization underlines its unique

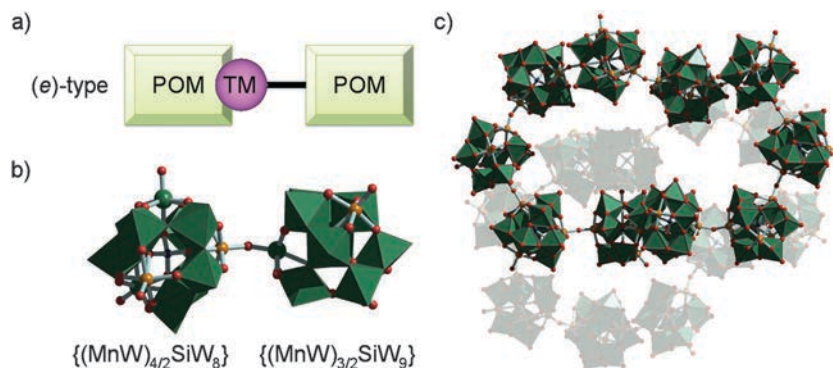


Fig. 23 (a) The fifth mode of framework connectivity, termed (e)-type, not covered by the four category model. Two TMSP units are connected at heterometal sites within the clusters, meaning no additional building blocks are required. (b) This particular example comprises trigonal $\{(MnW)_{3/2}SiW_9\}$ and tetrahedral $\{(MnW)_{4/2}SiW_8\}$ building blocks formed *in situ*.⁸⁷ (c) The three-dimensional Keggin network structure is formed by the extended connectivity of these building blocks.

nature, offering a great deal of potential for investigations of this new type of functional and responsive material.

The interesting observation in relation to this family of materials is that only one building block (the POM) is required. This means the Keggin framework structures comprise trigonal $\{(TMW)_{3/2}XW_9\}$ and tetrahedral $\{(TMW)_{4/2}XW_8\}$ building blocks, where TM = Mn or Co, and X = Si or Ge (Fig. 22 and 23).⁸⁷ In this case the building blocks are formed *in situ* and cannot be isolated as discrete clusters, however the TMs clearly occupy addenda sites of the parent Keggin unit. Although morpholine, an organic component, is required for formation of the network, it does not comprise an integral part of the scaffold. Instead, it resides in the framework pores in its protonated form (morpholinium), as a counter-cation to balance the negative charge on the framework. Reversible single-crystal to single-crystal transformations involving electronic switching of the TM centres have been demonstrated,⁸⁸ whilst alloy materials of the compound containing mixtures of Co and Mn have also been prepared.⁸⁹ The complete lack of a labile linker in (e)-type frameworks, such as the Keggin networks, ensures a robust framework capable of withstanding such physical and chemical transformations.

5.3 From well-defined intermediates (POM architectures) to materials

Ueda *et al.*, have studied a crystalline Mo_3VO_x ($x \leq 11.1$) mixed-metal-oxide that showed an outstanding catalytic activity for the selective oxidation of acrolein. The catalyst is synthesized from a solution containing pentagonal units of $\{Mo(Mo_5O_{27})\}$ which further react with molybdenum and vanadium species to form a 3D metal oxide, see Fig. 24.⁹⁰ In fact their building block assembly of a polyoxomolybdate has proven to be a successful strategy to form crystalline orthorhombic and trigonal MoV oxides.⁹¹ More specifically, the orthorhombic and trigonal MoV oxides were formed only from the precursor solution containing $\{Mo_{72}V_{30}\}$ Keplerate. These oxides contain the pentagonal Mo-based virtual building block in the crystal structure. Hydrothermal reaction of the precursor containing $\{Mo_{72}V_{30}\}$ produced crystalline orthorhombic or trigonal MoV oxides. Their results indicate that the pentagonal polyoxomolybdate unit produced

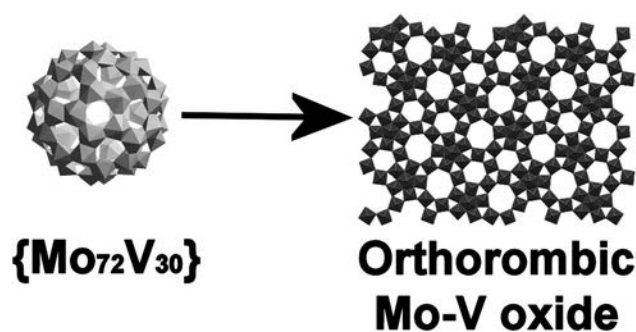


Fig. 24 Scheme showing the relationship between the precursor, $\{Mo_{72}V_{30}\}$ Keplerate and the formation of orthorhombic MoV oxide.

in the reaction precursor assembles with other Mo and V ions to form crystalline orthorhombic and trigonal MoV oxides.

In another recent paper a dipotassium diphosphatooctaper-oxotetramolybdate was isolated as a tetramethylammonium salt. The diphosphatomolybdate moieties are linked by potassium atoms to form an infinite anionic 1D double chain. The chains are linked to each other by hydrogen bonds to water molecules to form a 2D network, whilst the presence of potassium is essential to the synthesis of these present compound.⁹²

5.4 Ag-linked POM-OFs

An alternative approach for the preparation of functional extended solids involves the utilization of “softer” metallic linkers such as Ag^+ cations instead of transition metals or their complexes. The silver ion has attracted the attention of synthetic chemists due to their interesting chemistry and physical properties such as (a) its high affinity to N and O donors, (b) its numerous coordination numbers ranging from 2 to 9, (c) the $Ag \cdots Ag$ interactions and their associated properties, and (d) the cooperative effects between Ag-based aggregates and POMs which can lead to enhancement of catalytic efficacies or even emergence of new phenomena.⁹³ In this case the formation of the $Ag \cdots Ag$ interactions as well as the linking of the POM-based building blocks, is greatly depending on the appropriate choice

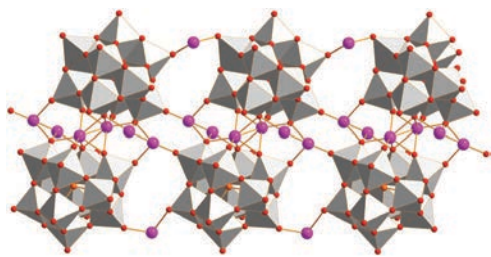


Fig. 25 Schematic representation of the $[PW_{11}O_{39}]$ -based extended architecture. The organic content have been omitted for clarity. Colour scheme: W, grey; Ag, pink; O, red.

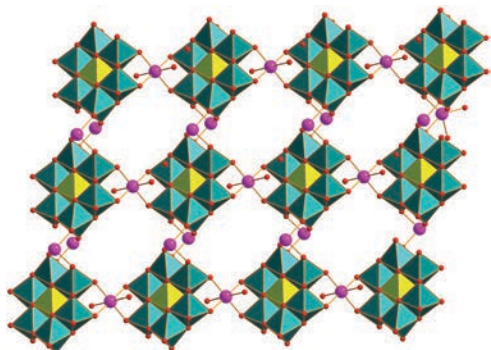


Fig. 26 Schematic representation of the Anderson POM-based hybrid architecture. The organic content have been omitted for clarity. Colour scheme: Mo, teal; Ag, pink; O, red; Al, light yellow.

of solvents or multidentate organic ligands such as triazoles and tetrazoles. To date, some Ag-POM based extended solids have been constructed. Amongst a few interesting examples is

the work reported in 2013 by Peng, Li *et al.*^{94a} where they prepared an α -Keggin-based polymer with multinuclear silver clusters, $\{[Ag_7(H_2biim)_5][PW_{11}O_{39}]\cdot Cl\cdot H_3O\}$ ($H_2biim = 2,29$ -biimidazole, $phnz = phenazine$), under hydrothermal conditions. X-ray diffraction analysis revealed a 2D network composed by dimerized monolacunary Keggin anions $\{PW_{11}O_{39}\}_2$ which are linked further together *via* pentanuclear silver clusters, see Fig. 25. Interestingly, X-ray diffraction analysis revealed that apart from the $\{Ag_5\}^{5+}$ cationic linkers, $\{Ag_4\}^{4+}$ clusters coexist in the structure which exhibit argentophilic interactions.

Another recent example, reported by An, Yin *et al.*^{94b} where in this case the use of carboxylates and Anderson type POMs, is depicted in Fig. 26, led to the formation of $[(3-Hpya)_2Ag] \cdot [(H_2O)_2Ag]_2[AlMo_6H_6O_{24}] \cdot 2H_2O$ (3-Hpya = 3-(3-pyridyl)acrylic acid). The compound exhibits a 2D network topology where the $[AlMo_6H_6O_{24}]^{3-}$ building blocks are linked together *via* Ag^+ cations and Ag-3-Hpya coordination complexes. Additionally, pyrolysis of this crystalline compounds gave rise to nanocomposite made of silver microparticles with different morphologies and excellent photocatalytic activity for the degradation of rhodamine B.

In a similar fashion, our group reported recently the complexation of small polyoxomolybdate cluster units with electrophilic silver centres to produce a new type of secondary building block in solution, constructed by β -octamolybdate clusters and $\{Ag_2\}$ dimers as linker groups. The assembly of this unprecedented building block can be directed by counterion and solvent interaction producing ultimately a series of compounds originating from a common building block library, and architectures ranging from isolated units, 1-D and 2-D topologies of $\{Ag(Mo_8O_{26})Ag\}$ based building blocks in the solid state. The structural diversity of this family of compounds is reflected in their dimensionality, in the coordination modes of the inorganic linkers $\{Ag_2\}$ as well as

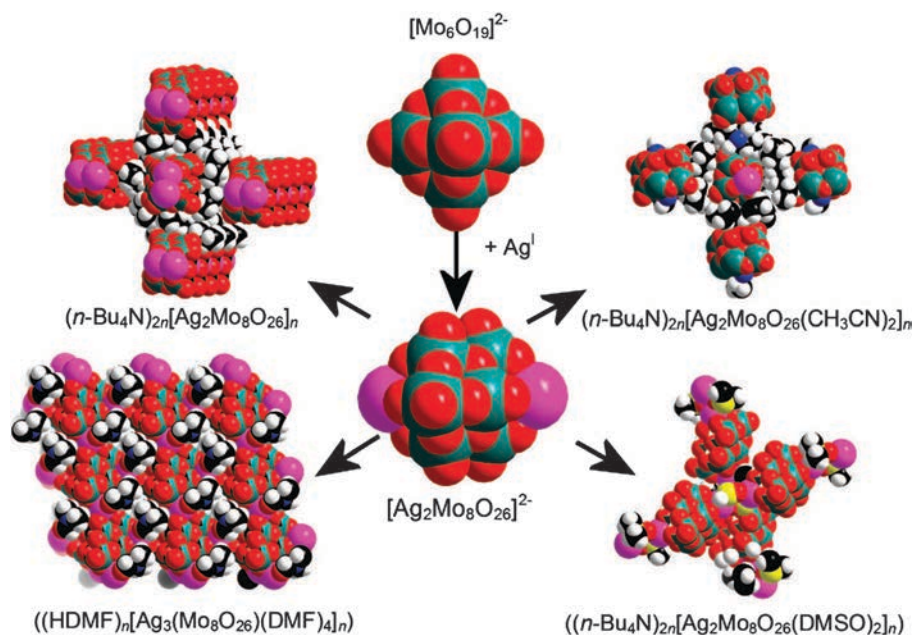


Fig. 27 Scheme showing the transformation of the Lindqvist anion, $[Mo_6O_{19}]^{2-}$, into the $[Ag_2Mo_8O_{26}]^{2-}$ building-block (centre) which subsequently forms a variety of POM cluster architectures in the solid state. Colour scheme: Mo, teal; Ag, pink; O, red; C, black; H, white; S, yellow.

in the nature of the Ag...Ag interactions that are present in most structures. The above synthetic approach was utilized successfully in the case of other inorganic linkers. In order to develop different synthetic approaches, the use of mass spectrometry has proven to be crucial to obtain key information; in terms of the speciation of the building block library as well as the real time monitoring of the assembly/speciation of the building blocks that give rise to the formation of a specific material. It is possible to use an organic cation exchange method with the purpose to investigate the assembly process of the well-known molybdenum Lindqvist, $[\text{Mo}_6\text{O}_{19}]^{2-}$, anion ($\{\text{Mo}_6\}$) in reactions with electrophilic silver(I) ions utilizing different chain lengths of alkylammonium salts. This investigation led to the isolation of a family of Ag-substituted, polymeric POM architectures consisting of β -octamolybdate, β - $[\text{Mo}^{\text{VI}}_8\text{O}_{26}]^{4-}$, ($\{\text{Mo}_8\}$) building-blocks linked through coordination to electrophilic silver(I) ions (Fig. 27).^{95–97}

Soft metals such, as silver has been particularly effective in linking together POM based clusters into arrays of coordination polymers with interesting topologies. For example, a range of diverse 1D, 2D and 3D infinite networks,⁹⁸ as well as discrete complexes⁹⁹ such as molecular grids, cages and helicates have been reported. The use of rigid, sterically bulky cations allowed us to achieve a high level of control over the constructed topologies. For example, the tetraphenylphosphonium ions in DMSO solvent allowed the isolation of the $(\text{Ph}_4\text{P})_2[\text{Ag}_2\text{Mo}_8\text{O}_{26}((\text{CH}_3)_2\text{SO})_4]$ which is composed of 'monomers' of the $(\text{Ag}\{\text{Mo}_8\}\text{Ag})$ building-block.⁹⁵ The variation of alkylammonium cation chain lengths, *i.e.* tetrapropyl-, tetrabutyl-, tetrahexyl-, and tetraheptylammonium ions in a range of organic media (CH_3CN , DMSO and DMF), led to the isolation of a variety of architectures ranging from chains, to grids and 2D-networks, see Fig. 28. The diversity of the obtained topologies was shown to be controlled mainly by the steric requirements of the organic cations or coordination ability of the solvent molecules.^{95,96} Another interesting feature is the uncommon for d^{10} (*i.e.* filled d-shell) bridging units which are held together by significant argentophilic interactions as well as additional stabilization offered by the $\{\text{Mo}_8\}$ cluster units.

In an effort to expand this interesting type of chemistry, our group demonstrated control over the molecular growth processes utilizing polyoxometalate-based building blocks with silver connecting units which led to the isolation of four new materials, $[\text{Ag}_3(\text{bhepH})_8(\text{W}_{11.5}\text{Na}_{0.5}\text{O}_{40}\text{P})_2]$ ($\text{bhep} = N,N'$ -bis(2-hydroxyethyl)piperazine); $[\text{Ag}_4(\text{DMSO})_8(\text{Mo}_8\text{O}_{26})_n]$; $\{\text{Ag}_3[\text{MnMo}_6\text{O}_{18}\{(\text{OCH}_2)_3\text{CNH}_2\}_2(\text{DMSO})_5]\}$; $\{\text{Ag}_3[\text{MnMo}_6\text{O}_{18}\{(\text{OCH}_2)_3\text{CNH}_2\}_2(\text{DMSO})_6(\text{CH}_3\text{CN})_2]\text{DMSO}\}_n$. These compounds range between 0D dimer connected by silver ions but was also found to form channels facilitated by the hydrogen bonding between the protonated $[\text{bhepH}]^+$ ligand and the cluster, 1D and 2D networks. The interesting observation is that these extended structures are all connected by Ag(I) ions.^{95,96} Furthermore it was shown that the stability of these materials was greatly influenced by the presence of the silver and solvent (DMSO) coordinating ligand rather than the structural features of the polyoxometalate building block. Additional surface studies of the deposition of the 1D and 2D compounds on silicon substrates yielded fibres $> 10 \mu\text{m}$ in length with a diameter of *ca.* $0.5 \mu\text{m}$.

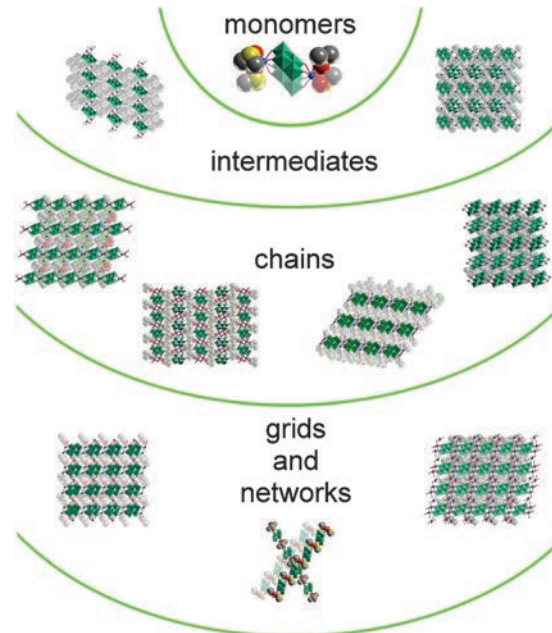


Fig. 28 A summary of the variety of silver-silver dimeric moieties stabilized by the β -octamolybdate cluster isolated when reacting $[\text{Mo}_6\text{O}_{19}]^{2-}$ anions with silver(I) cations in the presence of tetraphenylphosphonium cations or different chain length alkylammonium cations, and by varying the solvent system used.^{95,96} The 'monomer' ($\text{Ag}\{\text{Mo}_8\}\text{Ag}$) building block and the four coordinated DMSO solvent molecules of the compound $(\text{Ph}_4\text{P})_2[\text{Ag}_2\text{Mo}_8\text{O}_{26}((\text{CH}_3)_2\text{SO})_4]$ is shown at the top of this figure. The 'intermediates' section of the figure shows structures which are intermediate between the monomer and polymeric chain structures. The 'chains' section shows the structures composed of polymeric, infinite chains, where the silver cations engage in both the long range Ag-O contacts, and argentophilic interactions. The 'grids and networks' section illustrates the structures formed *via* further silver(I) cations coordinating between adjacent $(\text{Ag}\{\text{Mo}_8\}\text{Ag})_\infty$ chains. Colour scheme: Mo, teal polyhedra; Ag, blue; O, red; C, grey; S, yellow. Non-coordinating solvent molecules and H atoms are omitted for clarity.

Another example of Ag-based nanostructured composite materials involves the utilization of polyoxovanadate precursors. Indeed we showed that it is possible to embed $\{\text{Ag}_3\}$ and $\{\text{Ag}_1\}$ units, and $[\text{H}_2\text{V}_{10}\text{O}_{28}]^{4-}$ clusters, into supramolecular architectures, giving 1D zigzag chains and 2D networks, see Fig. 29.

More specifically, we discovered that the crystalline precursors could selectively be transformed into nanoscopic vanadium oxide wire-interpenetrated matrix decorated with metallic silver particles. This is an interesting finding with significant advantages over the existing nanowire/nanoparticle syntheses as it is an one-step process under mild conditions allowing the grafting of metal nanoparticles directly onto a catalytically active metal oxide nanowire matrix, see Fig. 30. The availability of transition metal POM compounds, with a wide range of architectures and properties, creates an opportunity for preparing complex nanostructured materials.^{100,101}

As we mentioned earlier the architecture of the POM-based building unit is crucial not only for the stability of the designed POM-OF but also of the observed structural features and potentially properties. This is a very rich area for the development

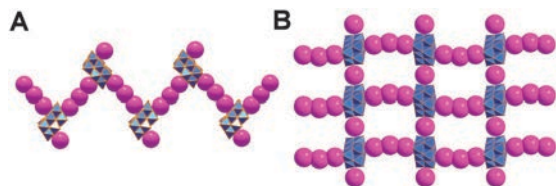


Fig. 29 Representation of the: (A) 1D zigzag chains formed by coordination of $\{Ag_3\}$ linker groups to adjacent faces of the $\{V_{10}\}$ clusters with capping $\{Ag_1\}_{cap}$ groups; (B) planar 2D network formed by $\{V_{10}\}$ clusters cross-linked by co-parallel $\{Ag_3\}$ primary linkers and secondary $\{Ag_1\}_{link}$ units, respectively. Color scheme: $\{V_{10}\}$: blue polyhedra, $\{Ag_3\}/\{Ag_1\}_{cap/link}$: pink spheres.

of assemblies and the use of non-coordinating/weakly complexing ligands for the preparation of novel materials. Another interesting prospect is the preparation of silver-tungsten-oxide frameworks, where different isomers of isopolyoxotungstate systems could be incorporated into highly connected framework materials using Ag(i) as a linking unit yielding extended solids with unique structural features. Further thermal treatment of the materials could lead to the formation of silver microparticles embedded in a tungsten oxide matrix. This novel synthetic approach promises to create a new class of nanostructured tungsten-silver-oxides with interesting physical properties, as well as a new example of a frameworks based upon

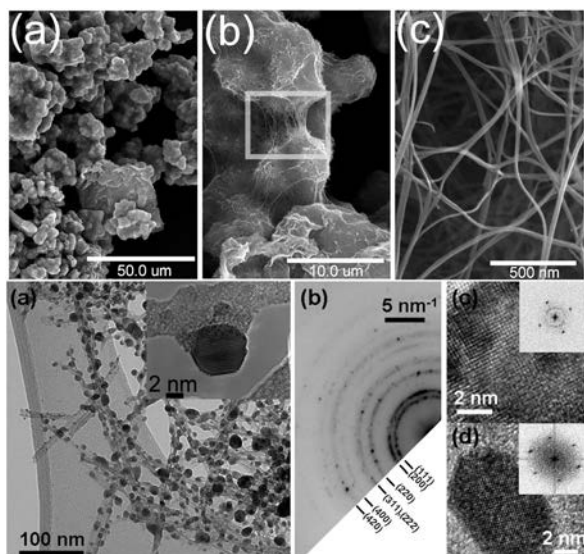


Fig. 30 Top: SEM micrographs of the nanowire structures in composite material. (a) Low magnification of the globular superstructures of cross-connected wires. (b) Detailed illustration of the wire superstructures which are connected by sections of aligned wires (highlighted by a grey rectangle). (c) High resolution of a globule section, showing the highly interweaved structure; Bottom: TEM and electron diffraction images of the composite nanowires. (a) Bright-field TEM of the composite Ag@VO_x wires and inset: HRTEM of an Ag nanoparticle embedded in the nanowire matrix. (b) Electron diffraction of a similar area, indicating rings consistent with the fcc Ag metal. (c) A typical region of the reduced vanadium matrix after exposure to the electron beam and (inset) Fourier transform consistent with a body-centered cubic (bcc) symmetry, giving a lattice constant of $a_v = 2.87 \text{ \AA}$. (d) A crystalline Ag nanoparticle and (inset) Fourier transform consistent with a face-centered cubic (fcc) symmetry and a lattice constant of $a_{Ag} = 3.91 \text{ \AA}$.

solution processable POM clusters.¹⁰² Based on the above, we utilized different isomers of the isopolyoxotungstate $\{W_{19}\}$ as building block and combined it with Ag(i) linkers, yielded compounds which have different structural properties as a function of the cluster isomer type, and the level of silver connectivity in the frameworks (Fig. 31 and 32). Not only does this work expanded the list of synthetic approaches used for the design of polyoxometalate based open frameworks (POM-OFs), eliminating the need for structure directing organic linkers, but also the use of silver acetonitrile complexes can be used effectively as structure directing cations allowing easy removal of the ligand-based solvent upon further processing of the material.

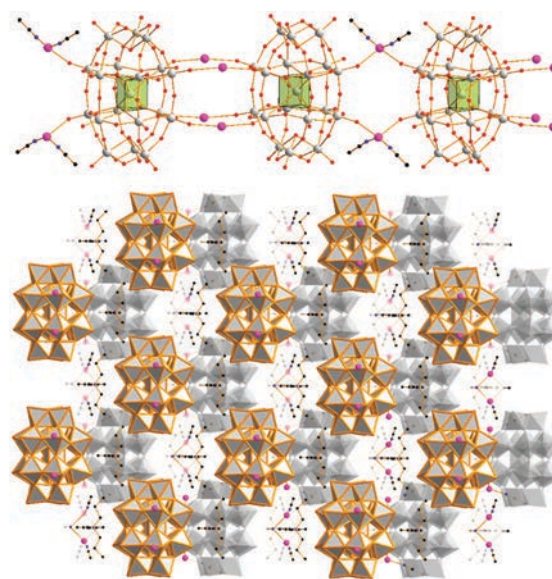


Fig. 31 Representation of the formed framework observed in $[(Ag(CH_3CN)_2)(CH_3CN)]\{\alpha-[H_4W_{19}O_{62}](TPA)_2(Ag(CH_3CN)_2)(Ag)_2\}\cdot 7(CH_3CN)$. Top: basic framework connectivity of the silver linked $\{\alpha-W_{19}\}$ clusters with the central tungsten prismatic geometry highlighted. Bottom: polyhedral representation of the extended framework shown along the crystallographic c-axis. W, grey polyhedra; O, red spheres; Ag, pink spheres; C, black spheres; N, blue spheres.

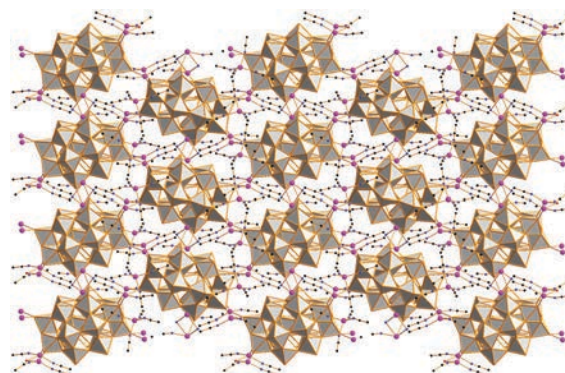


Fig. 32 Representation of the framework prepared using $\gamma^*\text{-}\{W_{19}\}$. Polyhedral representation of the crystal packing in the lattice viewing along the crystallographic a axis. W, grey polyhedra; O, red spheres; Ag, pink spheres; C, black spheres; N, blue spheres.

In fact, it may be appropriate to suggest that this approach might lead to a whole new class of nanostructured tungsten-silver-oxides with a range of interesting physical properties. Ongoing work in our group exploits the potential of these novel materials in areas like catalysis, antimicrobial materials, electroactive/photoactive coatings, and new design principles that utilize molecular precursors to produce pure heterometal oxide materials from solution processes.

6. Conclusions and outlook

In this review we have discussed the current state of the art where it comes to the development of new extended solids based upon polyoxometalate building blocks. Apart from the academic interest, the recent development of the field of POM-OFs is driven by the wide range of applications related to sensing and catalysis as well as to the emergence of functionality (*e.g.* molecular separation, selective catalysis, structure transformation *etc.*). The diverse family of POM-OF materials combine the advantages of POM chemistry with the properties of MOF chemistry. This means that the combination of mild synthetic conditions, wide range of structural motifs, porosity, high surface area and thermal stability together render them a promising new family of materials which offer the unique opportunity to design functionality. Furthermore, the interplay between the structure directing cations and the dual role offered by POMs (act as template and building block), as with the synthesis of zeolites, are vital for the formation of the framework whilst the wide range of reaction processing conditions allow for a wide variety of structure types and properties. Moreover, the mild synthetic conditions allows 'meta-stable' POMs to be trapped and utilised in frameworks that are quite stable and therefore this opens up a whole host of new and exciting design issues.

How can different functions be 'dialled-in' as a function of the kinetic trapping of the compound? Can external physical aspects be used to aid this process? How can the structure directing cations be removed or reduced in size post synthesis to increase the accessible pore space for host-guest interactions? Can frameworks using preformed pores, based upon giant ring shaped POMs be used make new materials? Can surface templates be used to nucleate POM 'framework' nano-crystals? How can we expand the number of sensible, designed, hypothesis driven assemblies beyond synthetically 'random' assemblies? In these respects the development of POM-OFs is sure to accelerate and we hope that researchers will consider these overarching questions in their quest to design and discover new POM-OFs.

Acknowledgements

The authors would like to thank The Glasgow University, EPSRC, Leverhulme Trust, the Royal Society, the Royal Society of Edinburgh and Marie Curie actions for financial support.

References

- 1 N. Mizuno and K. Kamata, *Coord. Chem. Rev.*, 2011, **255**, 2358.
- 2 T. Charles, *Coord. Chem. Rev.*, 1998, **178–180**(part 2), 1165.
- 3 L. E. Briand, G. T. Baronetti and H. J. Thomas, *Appl. Catal., A*, 2003, **256**, 37.
- 4 Q. Yin, J. M. Tan, C. Besson, Y. V. Geletii, D. G. Musaev, A. E. Kuznetsov, Z. Luo, K. I. Hardcastle and C. L. Hill, *Science*, 2010, **328**, 342.
- 5 E. Coronado, C. Giménez-Saiz and C. J. Gómez-García, *Coord. Chem. Rev.*, 2005, **249**, 1776.
- 6 H. Sung, H. So and W. K. Paik, *Electrochim. Acta*, 1994, **39**, 645.
- 7 J.-D. Compain, P. Mialane, A. Dolbecq, I. M. Mbomekallé, J. Marrot, F. Sécheresse, E. Rivière, G. Rogez and W. Wernsdorfer, *Angew. Chem., Int. Ed.*, 2009, **48**, 3077.
- 8 C. Ritchie, A. Ferguson, H. Nojiri, H. N. Miras, Y.-F. Song, D.-L. Long, E. Burkholder, M. Murrie, P. Kögerler, E. K. Brechin and L. Cronin, *Angew. Chem., Int. Ed.*, 2008, **47**, 5609.
- 9 C. R. Mayer, R. Thouvenot and T. Lalot, *Chem. Mater.*, 2000, **12**, 257.
- 10 E. Coronado and C. J. Gómez-García, *Chem. Rev.*, 1998, **98**, 273.
- 11 B. Hasenknopf, *Front. Biosci.*, 2005, **10**, 275.
- 12 J. T. Rhule, C. L. Hill, D. A. Judd and R. F. Schinazi, *Chem. Rev.*, 1998, **98**, 327.
- 13 M. T. Pope and A. Muller, *Angew. Chem., Int. Ed. Engl.*, 1991, **30**, 34.
- 14 Special issue on polyoxometalates, ed. C. L. Hill, *Chem. Rev.*, 1998, **98**, 1.
- 15 D.-L. Long, E. Burkholder and L. Cronin, *Chem. Soc. Rev.*, 2007, **36**, 105.
- 16 D.-L. Long, R. Tsunashima and L. Cronin, *Angew. Chem., Int. Ed.*, 2010, **49**, 1736.
- 17 (a) Special issue on polyoxometalates, ed. L. Cronin and A. Müller, *Chem. Soc. Rev.*, 2012, **41**, 7325; (b) H. N. Miras, J. Yan, D.-L. Long and L. Cronin, *Chem. Soc. Rev.*, 2012, **41**, 7403.
- 18 C. P. Pradeep, D.-L. Long and L. Cronin, *Dalton Trans.*, 2010, **39**, 9443.
- 19 A. Müller and P. Gouzerh, *Chem. Soc. Rev.*, 2012, **41**, 7431.
- 20 M. Hutin, D.-L. Long and L. Cronin, *Isr. J. Chem.*, 2011, **5**, 205.
- 21 L. Cronin, P. Kögerler and A. Müller, *J. Solid State Chem.*, 2000, **152**, 57.
- 22 (a) A. Müller, E. Beckmann, H. Bögge, M. Schmidtman and A. Dress, *Angew. Chem., Int. Ed.*, 2002, **41**, 1162; (b) H. N. Miras, C. J. Richmond, D.-L. Long and L. Cronin, *J. Am. Chem. Soc.*, 2012, **134**, 3816; (c) H. N. Miras, G. J. T. Cooper, D. L. Long, H. Bögge, A. Müller, C. Streb and L. Cronin, *Science*, 2010, **327**, 72.
- 23 (a) L. Cronin, *Compr. Coord. Chem. II*, Elsevier, Amsterdam, 2004, vol. 7; (b) A. Müller and P. Kögerler, *Coord. Chem. Rev.*, 1999, **182**, 3.
- 24 N. Fay, A. M. Bond, C. Baffert, J. F. Boas, J. R. Pillbrow, D.-L. Long and L. Cronin, *Inorg. Chem.*, 2007, **46**, 3502.

- 25 (a) B. Dawson, *Acta Crystallogr., Sect. B: Struct. Crystallogr. Cryst. Chem.*, 1953, **6**, 113; (b) R. Strandberg, *Acta Chem. Scand., Ser. A*, 1975, **29a**, 350.
- 26 L. Cronin, in *Comprehensive Coordination Chemistry II: From Biology to Nanotechnology*, ed. J. A. McCleverty and T. J. Meyer, Elsevier, Amsterdam, 2004, vol. 7.
- 27 B. Godin, Y.-G. Chen, J. Vaissermann, L. Ruhlmann, M. Verdauger and P. Gouzerh, *Angew. Chem., Int. Ed.*, 2005, **44**, 3072.
- 28 Z. Zhang, Y. Li, Y. Wang, Y. Qi and E. Wang, *Inorg. Chem.*, 2008, **47**, 7615.
- 29 B. Godin, J. Vaissermann, P. Herson, L. Ruhlmann, M. Verdauger and P. Gouzerh, *Chem. Commun.*, 2005, 5624.
- 30 S. Yao, Z. Zhang, Y. Li and E. Wang, *Dalton Trans.*, 2010, **39**, 3884.
- 31 X. Fang, P. Kögerler, Y. Furukawa, M. Speldrich and M. Luban, *Angew. Chem., Int. Ed.*, 2011, **50**, 5212.
- 32 C. J. Richmond, H. N. Miras, A. R. de la Oliva, H. Zang, V. Sans, L. Paramonov, C. Makatsoris, R. Inglis, E. K. Brechin, D.-L. Long and L. Cronin, *Nat. Chem.*, 2012, **4**, 1037.
- 33 L. Vilà-Nadal, S. G. Mitchell, S. Markov, C. Busche, V. Georgiev, A. Asenov and L. Cronin, *Chem. – Eur. J.*, 2013, **19**, 16502.
- 34 L. Vilà-Nadal, K. Peuntinger, C. Busche, J. Yan, D. Lüders, D.-L. Long, J. M. Poblet, D. M. Guldi and L. Cronin, *Angew. Chem., Int. Ed.*, 2013, **52**, 9695.
- 35 J. A. Fernández, X. López, C. Bo, C. de Graaf, E. J. Baerends and J.-M. Poblet, *J. Am. Chem. Soc.*, 2007, **129**, 12244.
- 36 J. Y. Kempf, M.-M. Rohmer, J.-M. Poblet, C. Bo and M. Bénard, *J. Am. Chem. Soc.*, 1992, **114**, 1136.
- 37 (a) X. López, J. J. Carbó, C. Bo and J.-M. Poblet, *Chem. Soc. Rev.*, 2012, **41**, 7537; (b) L. Vilà-Nadal, S. G. Mitchell, D.-L. Long, A. Rodríguez-Fortea, X. López, J. M. Poblet and L. Cronin, *Dalton Trans.*, 2012, **41**, 2264; (c) J. M. Cameron, J. Gao, L. Vilà-Nadal, D.-L. Long and L. Cronin, *Chem. Commun.*, 2014, **50**, 2155.
- 38 T. R. Cook, Y.-R. Zheng and P. J. Stang, *Chem. Rev.*, 2013, **113**, 734.
- 39 B. Godin, J. Vaissermann, P. Herson, L. Ruhlmann, M. Verdaguer and P. Gouzerh, *Chem. Commun.*, 2005, 5624.
- 40 S. Yao, Z. M. Zhang, Y. G. Li and E. Wang, *Dalton Trans.*, 2009, 1786.
- 41 Y. W. Li, Y. H. Wang, X. J. Feng, Y. Lu and E. B. Wang, *Inorg. Chem.*, 2009, **48**, 6452.
- 42 B. Godin, Y. G. Chen, J. Vaissermann, L. Ruhlmann, M. Verdaguer and P. Gouzerh, *Angew. Chem., Int. Ed.*, 2005, **44**, 3072.
- 43 F. Hussain, U. Kortz, B. Keita, L. Nadjó and M. T. Pope, *Inorg. Chem.*, 2006, **45**, 761.
- 44 L. Pauling, *The Nature of the Chemical Bond and the Structure of Molecules and Crystals*, Cornell University Press, Ithaca, N.Y., 2nd edn, 1945, p. 378.
- 45 G. R. Desiraju, *Nature*, 2000, **408**, 407.
- 46 J. Wu, G. Hu, P. Wang, F. Hao, H. Zhou, A. Zhou, Y. Tian and B. Jin, *Dyes Pigm.*, 2011, **88**, 174.
- 47 T. Akutagawa, D. Endo, S.-I. Noro, L. Cronin and T. Nakamura, *Coord. Chem. Rev.*, 2007, **251**, 2547.
- 48 S.-X. Guo, J. Xie, R. Gilbert-Watson, S. L. Birkett, A. M. Bond and A. G. Wedd, *Dalton Trans.*, 2011, **40**, 356.
- 49 S. Uchida, M. Hashimoto and N. Mizuno, *Angew. Chem., Int. Ed.*, 2002, **41**, 2814.
- 50 S. Uchida and N. Mizuno, *J. Am. Chem. Soc.*, 2004, **126**, 1602.
- 51 S. Uchida and N. Mizuno, *Coord. Chem. Rev.*, 2007, **251**, 2537.
- 52 S. Uchida, R. Kawamoto, T. Akatsuka, S. Hikicha and N. Mizuno, *Chem. Mater.*, 2005, **17**, 1367.
- 53 R. Kawamoto, S. Uchida and N. Mizuno, *J. Am. Chem. Soc.*, 2005, **127**, 10560.
- 54 S. Uchida, A. Lesbani, Y. Ogasawara and N. Mizuno, *Inorg. Chem.*, 2012, **51**, 775.
- 55 K. Suzuki, Y. Kikukawa, S. Uchida, H. Tokoro, K. Imoto, S.-I. Ohkoshi and N. Mizuno, *Angew. Chem., Int. Ed.*, 2012, **51**, 1597.
- 56 L. Cronin, P. Kögerler and A. Müller, *J. Solid State Chem.*, 2000, **152**, 57.
- 57 Y. Wang, L. Ye, T.-G. Wang, X.-B. Cui, S.-Y. Shi, G.-W. Wang and J. Q. Xu, *Dalton Trans.*, 2010, **39**, 1916.
- 58 A. Proust, R. Thouvenot and P. Gouzerh, *Chem. Commun.*, 2008, 1837.
- 59 A. Dolbecq, E. Dumas, C. R. Mayer and P. Mialane, *Chem. Rev.*, 2010, **110**, 6009.
- 60 D. E. Katsoulis, *Chem. Rev.*, 1998, **98**, 359.
- 61 M. Lu, Y. Wei, B. Xu, C. F.-X. Cheung, Z. Peng and D. R. Powell, *Angew. Chem., Int. Ed.*, 2002, **41**, 1566.
- 62 J. L. Stark, A. L. Rheingold and E. Maatta, *J. Chem. Soc., Chem. Commun.*, 1995, 1165.
- 63 H. Zeng, G. R. Newkome and C. L. Hill, *Angew. Chem., Int. Ed.*, 2000, **39**, 1771.
- 64 (a) P. Judenstein, *Chem. Mater.*, 1992, **4**, 4; (b) C. R. Mayer, R. Thouvenot and T. Lalot, *Chem. Mater.*, 2000, **12**, 257; (c) R. C. Schroden, C. F. Blanford, B. J. Melde, B. J. S. Johnson and A. Stein, *Chem. Mater.*, 2001, **3**, 1074; (d) C. Sanchez, G. J. de A. A. Soller-Illia, F. Ribot, T. Lalot, C. R. Mayer and V. Cabuil, *Chem. Mater.*, 2001, **13**, 3061 and references therein.
- 65 (a) C.-M. Liu, D.-Q. Zhang, M. Xiong and D.-B. Zhu, *Chem. Commun.*, 2002, 1416; (b) J.-Y. Niu, Q. Wu and J.-P. Wang, *J. Chem. Soc., Dalton Trans.*, 2002, 2512; (c) W.-M. Bu, L. Ye, G.-Y. Yang, J.-S. Gao, Y.-G. Fan, M.-C. Shao and J.-Q. Xu, *Inorg. Chem. Commun.*, 2001, **4**, 1; (d) M. I. Khan, *J. Solid State Chem.*, 2000, **152**, 105 and references therein; (e) D. J. Chesnut, D. Hagrman, P. J. Zapf, R. P. Hammond, R. Laduca, R. C. Haushalter and J. Zubieta, *Coord. Chem. Rev.*, 1999, **192**, 737; (f) A. Müller, M. Koop, P. Schiffels and H. Bögge, *J. Chem. Soc., Chem. Commun.*, 1997, 1715; (g) J. R. D. Debord, R. C. Haushalter, L. M. Meyer, D. J. Rose, P. J. Zapf and J. Zubieta, *Inorg. Chim. Acta*, 1997, **256**, 165; (h) I. Loose, M. Bösing, R. Klein, B. Krebs, R. P. Schultz and B. Scharbert, *Inorg. Chim. Acta*, 1997, **263**, 99; (i) J. Galan-Mascaros, C. Gimenez-Saiz, S. Tricki, C. J. Gomez-Garcia, E. Coronado and L. Ouahab, *Angew. Chem.*, 1995, **107**, 1601 (*Angew. Chem., Int. Ed. Engl.*, 1995,

- 34, 1460); (j) C. Gimenez-Saiz, J. R. Galan-Mascaros, S. Tricky, E. Coronado and L. Ouahab, *Inorg. Chem.*, 1995, **34**, 524.
- 66 (a) A. Dolbecq, P. Mialane, L. Lisnard, J. Marrot and F. Sécheresse, *Chem. – Eur. J.*, 2003, **9**, 2914; (b) A. Dolbecq, C. Mellot-Draznieks, P. Mialane, J. Marrot, G. Férey and F. Sécheresse, *Eur. J. Inorg. Chem.*, 2005, 3009; (c) C. Lei, J.-G. Mao, Y.-Q. Sun and J.-L. Song, *Inorg. Chem.*, 2004, **43**, 1964.
- 67 W. Wang, L. Xu, G. Gao, L. Liu and X. Liu, *CrystEngComm*, 2009, **11**, 2488.
- 68 B. Nohra, H. El Moll, L. M. R. Albelo, P. Mialane, J. Marrot, C. Mellot-Draznieks, M. O’Keeffe, R. N. Biboum, J. Lemaire, B. Keita, L. Nadjo and A. Dolbecq, *J. Am. Chem. Soc.*, 2011, **133**, 13363.
- 69 L. M. R. Albelo, A. R. Ruiz-Salvador, D. W. Lewis, A. Gómez, P. Mialane, J. Marrot, A. Dolbecq, A. Sampierie and C. Mellot-Draznieks, *Phys. Chem. Chem. Phys.*, 2010, **12**, 8632.
- 70 S.-T. Zheng, J. Zhang and G.-Y. Yang, *Angew. Chem., Int. Ed.*, 2008, **47**, 3909.
- 71 X. Wang, H. Hu, B. Chen, H. Lin, A. Tian and J. Li, *Solid State Sci.*, 2003, **5**, 1177.
- 72 J. Song, Z. Luo, D. K. Britt, H. Furukawa, O. M. Yaghi, K. I. Hardcastle and C. L. Hill, *J. Am. Chem. Soc.*, 2011, **133**, 16839.
- 73 H. Zhang, L. Duan, Y. Lan, E. Wang and C. Hu, *Inorg. Chem.*, 2003, **42**, 8053.
- 74 C. Zou, Z. Zhang, X. Xu, Q. Gong, J. Li and C.-D. Wu, *J. Am. Chem. Soc.*, 2012, **134**, 87.
- 75 J. Lü, J.-X. Lin, X.-L. Zhao and R. Cao, *Chem. Commun.*, 2012, **48**, 669.
- 76 C.-M. Liu, D.-Q. Zhang, M. Xiong and D.-B. Zhu, *Chem. Commun.*, 2002, 1416.
- 77 S. Reinoso, P. Vitoria, L. Lezama, A. Luque and J. M. Gutiérrez-Zorrilla, *Inorg. Chem.*, 2003, **42**, 3709.
- 78 D. Dutta, A. D. Jana, M. Debnath, A. Bhaumik, J. Marek and M. Ali, *Dalton Trans.*, 2010, **39**, 11551.
- 79 M. I. Khan, E. Yohannes and R. J. Doedens, *Angew. Chem., Int. Ed.*, 1999, **38**, 1292.
- 80 K. Okamoto, S. Uchida, T. Ito and N. Mizuno, *J. Am. Chem. Soc.*, 2007, **129**, 7378.
- 81 B. S. Bassil, M. Ibrahim, S. S. Mal, A. Suchopar, R. N. Biboum, B. Keita, L. Nadjo, S. Nellutla, J. van Tol, N. S. Dalal and U. Kortz, *Inorg. Chem.*, 2010, **49**, 4949.
- 82 S. G. Mitchell, D. Gabb, C. Ritchie, N. Hazel, D.-L. Long and L. Cronin, *CrystEngComm*, 2009, **11**, 36.
- 83 L.-C. Zhang, H. Xue, Z.-M. Zhu, Z.-M. Zhang, Y.-G. Li and E.-B. Wang, *J. Cluster Sci.*, 2010, **21**, 679.
- 84 S. G. Mitchell, T. Boyd, H. N. Miras, D.-L. Long and L. Cronin, *Inorg. Chem.*, 2011, **50**, 136.
- 85 S.-W. Chen, K. Boubekour, P. Gouzerh and A. Proust, *J. Mol. Struct.*, 2011, **994**, 104.
- 86 S. G. Mitchell, C. Streb, H. N. Miras, T. Boyd, D.-L. Long and L. Cronin, *Nat. Chem.*, 2010, **2**, 308.
- 87 C. Ritchie, C. Streb, J. Thiel, S. G. Mitchell, H. N. Miras, D.-L. Long, T. Boyd, R. D. Peacock, T. McGlone and L. Cronin, *Angew. Chem., Int. Ed.*, 2008, **47**, 6881.
- 88 J. Thiel, C. Ritchie, C. Streb, D.-L. Long and L. Cronin, *J. Am. Chem. Soc.*, 2009, **131**, 4180.
- 89 J. Thiel, C. Ritchie, H. N. Miras, C. Streb, S. G. Mitchell, T. Boyd, M. N. C. Ochoa, M. H. Rosnes, J. McIver, D.-L. Long and L. Cronin, *Angew. Chem., Int. Ed.*, 2010, **49**, 6984.
- 90 M. Sadakane, K. Endo, K. Kodato, S. Ishikawa, T. Murayama and W. Ueda, *Eur. J. Inorg. Chem.*, 2013, 1731.
- 91 M. Sadakane, N. Watanabe, T. Katou, Y. Nodasaka and W. Ueda, *Angew. Chem., Int. Ed.*, 2007, **46**, 1493.
- 92 K. Aoki, K. Iwata, T. Iwata and M. Hashimoto, *Eur. J. Inorg. Chem.*, 2013, 1808.
- 93 Y. Kikukawa, Y. Kuroda, K. Yamaguchi and N. Mizuno, *Angew. Chem., Int. Ed.*, 2012, **51**, 2434.
- 94 (a) Z.-Y. Shi, J. Peng, Y.-G. Li, Z.-Y. Zhang, X. Yu, K. Alimajea and X. Wang, *CrystEngComm*, 2013, **15**, 7583; (b) Y. Hu, H. An, X. Liu, J. Yin, H. Wang, H. Zhanga and L. Wang, *Dalton Trans.*, 2014, **43**, 2488.
- 95 H. Abbas, A. L. Pickering, D.-L. Long, P. Kögerler and L. Cronin, *Chem. – Eur. J.*, 2005, **11**, 1071.
- 96 H. Abbas, C. Streb, A. L. Pickering, A. R. Neil, D.-L. Long and L. Cronin, *Cryst. Growth Des.*, 2008, **8**, 635.
- 97 S. M. Chen, C. Z. Lu, Y. Q. Yu, Q. Z. Zhang and X. He, *Inorg. Chem. Commun.*, 2004, **7**, 1041.
- 98 1D: M. Fujita, Y. J. Kwon, O. Sasaki, K. Yamaguchi and K. Ogura, *J. Am. Chem. Soc.*, 1995, **117**, 7287; B. F. Hoskins, R. Robson and D. A. Slizys, *J. Am. Chem. Soc.*, 1997, **119**, 2952; 2D: L. Carlucci, G. Ciani, D. M. Proserpio and A. Sironi, *Angew. Chem., Int. Ed. Engl.*, 1996, **35**, 1088; C. V. K. Sharma and M. J. Zaworotko, *Chem. Commun.*, 1996, 2655; 3D: L. Carlucci, G. Ciani, D. M. Proserpio and A. Sironi, *Chem. Commun.*, 1996, 1393; B. F. Abrahams, S. R. Batten, H. Hamit, B. F. Hoskins and R. Robson, *Chem. Commun.*, 1996, 1313.
- 99 S. Ottens-Hildebrandt, S. Meier, W. Schmidt and F. Vögtle, *Angew. Chem., Int. Ed. Engl.*, 1994, **33**, 1767 and references therein.
- 100 E. F. Wilson, H. Abbas, B. J. Duncombe, C. Streb, D.-L. Long and L. Cronin, *J. Am. Chem. Soc.*, 2008, **130**, 13876.
- 101 C. Streb, R. Tsunashima, D. A. MacLaren, T. McGlone, T. Akutagawa, T. Nakamura, A. Scandurra, B. Pignataro, N. Gadegaard and L. Cronin, *Angew. Chem., Int. Ed.*, 2009, **48**, 6490.
- 102 T. McGlone, C. Streb, D.-L. Long and L. Cronin, *Adv. Mater.*, 2010, **22**, 4275.